SP-1279 (4)
April 2004

EarthCARE - Earth Clouds, Aerosols and Radiation Explorer
SPECTRA - Surface Processes and Ecosystem Changes Through Response Analysis
WALES - Water Vapour Lidar Experiment in Space
ACE+ - Atmosphere and Climate Explorer
EGPM - European Contribution to Global Precipitation Measurement
Swarm - The Earth's Magnetic Field and Environment Explorers

European Space Agency
Agence spatiale européenne

REPORTS FOR MISSION SELECTION
THE SIX CANDIDATE EARTH EXPLORER MISSIONS

ESA SP-1279(4)
April 2004

REPORTS FOR MISSION SELECTION
THE SIX CANDIDATE EARTH EXPLORER MISSIONS

ACE+ – Atmosphere and Climate Explorer

European Space Agency
Agence spatiale européenne

ESA SP-1279(4) – ACE+ – Atmosphere and Climate Explorer

Report prepared by: Mission Experts Division
Scientific Co-ordinator: T. Wehr

Published by: ESA Publications Division
c/o ESTEC, Noordwijk, The Netherlands
Editor: B. Battrick

ISBN 92-9092-962-6
ISSN 0379-6566

Price (6 vols): € 50

Contents

1. Introduction

The ESA Living Planet Programme includes two types of complementary user driven missions: the research-oriented Earth Explorer missions and the operational service oriented Earth Watch missions. These missions are implemented through the Earth Observation Envelope Programme (EOEP) and the Earth Watch Programme, where the Earth Explorer missions are completely covered by the EOEP.

Earth Explorer missions are divided into two classes, with Core missions being larger missions addressing complex issues of wide scientific interest, and Opportunity missions, which are smaller in terms of cost to ESA and address more limited issues. Both types of missions address the research objectives set out in the Living Planet Programme document (ESA SP-1227 1998), which describes the plans for the Agency's strategy for Earth Observation in the post-2000 time frame. All Earth Explorer missions are proposed, defined, evaluated and recommended by the scientific community.

Following a call for Core mission ideas in 2000 and selection of five of the ten proposals for pre-feasibility study, three of the candidates, EarthCARE, SPECTRA and WALES, were chosen for feasibility study in November 2001. In response to a call for Opportunity mission proposals in 2001, which resulted in 25 full proposals being submitted by early 2002, three mission candidates, ACE+, EGPM and SWARM, were also chosen for feasibility study. The Phase-A studies for all six Earth Explorer candidate missions are being finalised by early 2004, forming the basis for the Reports for Mission Selection for all six candidate missions.

The ACE+ candidate mission is based on the mission proposal co-written and submitted in 2002 by a team of scientific investigators led by Per Høeg (Danish Meteorological Institute, Copenhagen, Denmark) and Gottfried Kirchengast (University of Graz, Austria). This Report for Mission Selection was prepared based on inputs from the Mission Advisory Group (MAG) consisting of: S. Bühler (University of Bremen, Germany), K. Craig (Rutherford Appleton Laboratory, Didcot, UK), G. Elgered (Chalmers University of Technology, Onsala, Sweden), P. Høeg (Danish Meteorological Institute, Copenhagen, Denmark), G. Kirchengast (University of Graz, Austria), L. Kornblüh (Max-Planck Institute for Meteorology, Hamburg, Germany), H. Le Treut (Laboratoire de Météorologie Dynamique du CNRS, Paris, France). Parts of the Report have been prepared by the Executive based on inputs provided by the industrial Phase-A contractors. Others who, in various ways, have contributed to the Report are the Colleagues at IGAM, University of Graz, Austria and members of the teams of the system simulator and science performance studies (‘ACEPASS’ and ‘ACECLIM’).

The Report for Mission Selection for ACE+, together with those for the other five Earth Explorer candidate missions, is being circulated within the Earth Observation research community in preparation for a User Consultation Meeting at ESRIN, Frascati, Italy, in April 2004.

2. Background and Scientific Justification

Climate variations over the last 1000 years, as characterized by the mean global surface temperatures, have been confined within a range of about half a degree. The twentieth century has been mostly characterized by a warming trend, which tends to exceed those bounds. The latest IPCC scientific assessment report (IPCC 2001) concluded that, whereas the largest part of the observed global warming up to the fifties was probably due to natural processes, such as solar and internal climate variability, the warming during recent decades cannot be explained without a significant contribution from the increased concentration of greenhouse gases, caused by human activity. This conclusion originates from coupled atmosphere-ocean model simulations and the analysis of past climatic data.

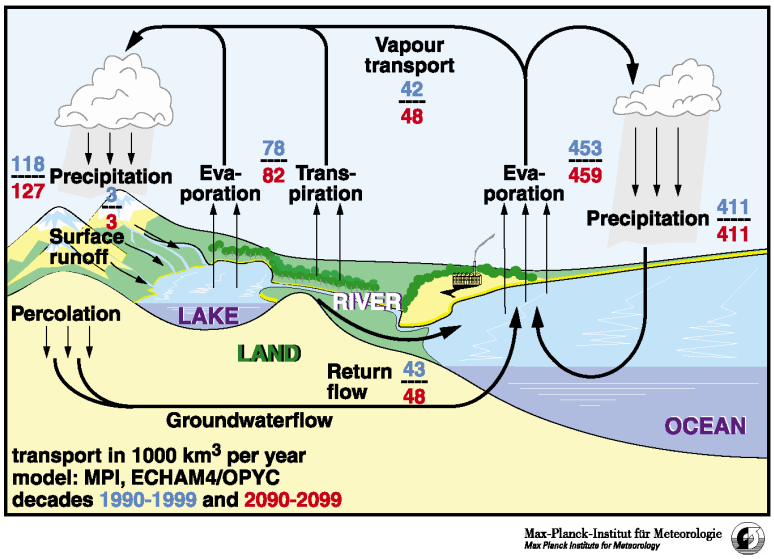

Figure 2.1: *The hydrological cycle based on a coupled climate model simulation for a doubling of CO_2 IPCC scenario (SRESa2) with ECHAM4/OPYC (MPIfM 2004).*

Climate model estimates of the hydrological cycle show that the humidity changes in the free troposphere are in the order of 15% (Fig. 2.1). The two established humidity data sets for global climate research are synoptic radiosonde records and records from the vertical sounding instruments (TOVS) of operational meteorological satellites. Between those two datasets a bias of approximately 10% relative humidity exists for the upper troposphere. To date, it has not been possible to verify which data set is closest to the truth (Soden and Lanzante 1996).

As pointed out in the IPCC report, water vapour feedback, e.g. the water vapour increase likely to occur in response to global warming, may double the warming resulting from any climate scenario, as can be assessed from a model simulation with fixed water vapour amounts. This effect further amplifies the other feedbacks, such as the cloud and ice albedo feedbacks. For example, a strong positive cloud feedback

would lead to 3.5 times greater warming compared to a fixed water vapour scenario. Hall and Manabe (1999) have also shown that these effects are necessary to explain the amplitude of natural climate fluctuations. Because of the coupling of humidity concentrations to the atmospheric temperature field by dynamics and thermodynamics, humidity feedback may act to amplify or attenuate other climate forcings (Harries 1997).

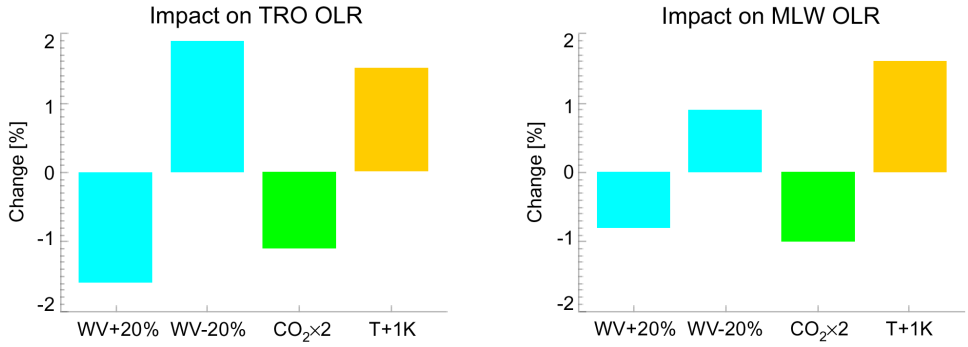

Figure 2.2: *Change in outgoing long-wave radiation (OLR) due to a 20% change in the absolute water vapour concentration throughout the column, a CO_2 doubling, and a 1 K increase in temperature. The left plot is for tropical (TRO) conditions, the right plot for a mid-latitude winter (MLW) scenario. An increase in the water vapour concentration will lead to an increase in absorption. This will shift the area of emission higher up in the troposphere to colder temperatures, thus reducing the OLR. An increase in the CO_2 concentration will block radiation, thus reducing the OLR and heating. A 1 K increase in temperature will increase the OLR (Courtesy of University of Bremen).*

The radiative effect of water vapour in comparison to that of carbon dioxide is shown in Figure 2.2. For a tropical atmosphere, a 20% increase in humidity has a larger climate impact than a doubling of the CO_2 concentration. The altitude region where the radiative effect of water vapour is most crucial is the free troposphere from approximately 2 to 10 km, as demonstrated by Figure 2.3. Traditional humidity measurement techniques perform poorly at the upper end of this altitude range. Thus the lack of high quality humidity data is one of the main reasons why the magnitude of the water vapour feedback in the upper troposphere remains a controversial issue (Kley and Russel, 1999).

It is the primary scientific goal of ACE+ to establish accurate tropospheric and lower stratospheric climatologies of humidity and temperature as two of the most important atmospheric parameters for climate research.

2.1 Trend Observations

The need to quantify variations and changes in climate results in the requirement for high-quality data sets, in particular for temperature and water vapour. Climate variations can be due to processes internal to the climate system, as well as to external

forcing effects. No anomalous forcing is needed to initiate internal climate variability, which basically occurs because of the differential radiative heating between high and low latitudes. Externally forced variations and changes, on the other hand, are due to anomalous influences such as change in the solar radiation, volcanic eruptions, or increased greenhouse effect.

Existing data sets, particularly for water vapour, are likely to have time-dependent biases and regional variations in trends. For humidity specifically, the available measurements in the upper troposphere and lower stratosphere (UTLS) were critically evaluated and summarized by the SPARC Project of the World Climate Research Programme (SPARC 2000). For the stratosphere, the conclusion is that an increase in the water vapour content has occurred, from 2-4 ppmv in the 1950s to present-day values of 4-6 ppmv. Half of this observed increase is not well understood.

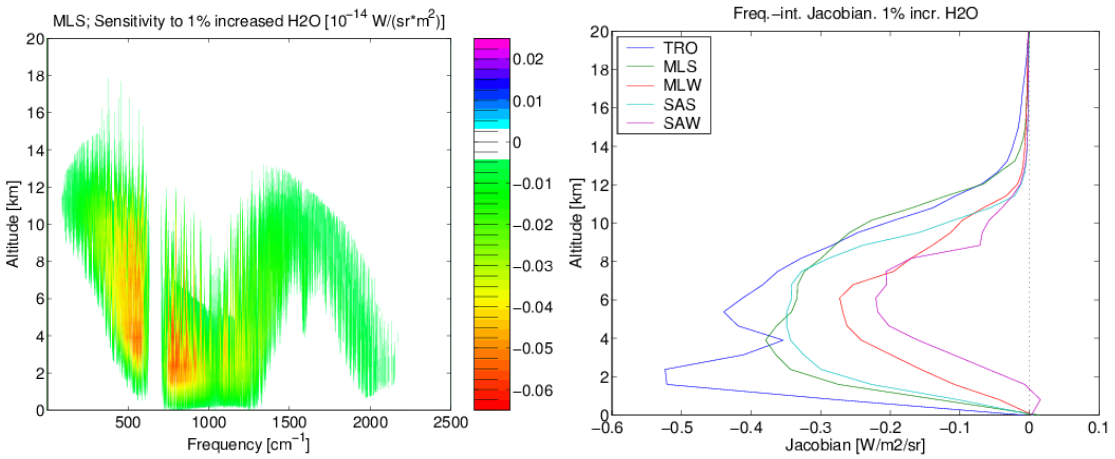

Figure 2.3: *Left plot: Top of the atmosphere radiation Jacobian with respect to water vapour, calculated with the radiative transfer model ARTS for a mid-latitude summer (MLS) scenario. Units are such that the Jacobian corresponds to the change in radiation intensity for a 1% increase in the water vapour in approximately a one-kilometre layer. The main area of sensitivity is at frequencies between 400 and 1000 cm^{-1} and altitudes between 2 and 10 km.*
Right plot: The same integrated in frequency, yielding the Jacobian of OLR. Different curves correspond to different atmospheric scenarios from tropical (TRO) to sub-arctic winter (SAW). This confirms the great importance of upper tropospheric humidity between approximately 4 and 10 km (Courtesy of University of Bremen).

The water vapour in the upper troposphere has been monitored for approximately 20 years using satellite instruments, although with poor accuracy. These data show significant long-term trends, both positive and negative, in different latitude areas, but no global trend has been detected. The self-calibrating nature of the ACE+ radio occultation observations would allow accurate tracking of changes in atmospheric water vapour content on short and long time scales, as already demonstrated with the GNSS-LEO observations (Leroy 1997, Schrøder et al. 2003).

TIROS Operational Vertical Sounder (TOVS) data, from the High Resolution Infrared Sounder (HIRS), have been the most important for monitoring the upper troposphere water vapour because of its long time series. The Microwave Limb Sounder (MLS) has been used to validate TOVS data. However, high spatial and temporal variability has made direct comparisons difficult, although monthly averages produce comparable results (Schrøder et al. 2003).

The SPARC report also comes to the conclusion that the operational radiosonde network offers neither an acceptable accuracy for the validation of other sensors, nor sufficient stability to be useful for long term monitoring of water vapour in the UTLS. According to SPARC (2000) recommendations, 'Upper tropospheric specific humidity should be monitored with a view to determining long-term variations. It is important to have complementary observations, not relying solely on one instrument or approach'.

2.2 Understanding and Prediction of Climate

Identifying and quantifying the water vapour, cloudiness, and temperature lapse rate feedback processes is a necessary objective to narrow the range of uncertainties that affect current climate models (Bony et al. 1997). For applications related to cloud microphysics, the important humidity parameter is relative humidity, not absolute humidity. For example, how much over-saturation of humidity with respect to ice is present in the upper troposphere is currently an active area of research (Spichtinger et al. 2002). In general, the use of remote sensing data, which do not provide consistent water vapour and temperature information, is problematic for such studies, since uncertainties in the atmospheric temperature propagate strongly into uncertainties in the retrieved relative humidity, as shown in (Buehler and Courcoux 2003). It is easy to show that a standard deviation of 1 K on the temperature measurement will lead to a standard deviation of around 13% on the relative humidity, ignoring all other sources of error (for 100% true relative humidity and a temperature of 220 K).

Water vapour has a short residence time in the atmosphere. As a result, its distribution over the globe is very uneven, and depends on a large number of complex processes. This, together with the limitations in present observing systems, makes it still poorly quantified and modelled with insufficient accuracy in global circulation models. As a consequence, the whole hydrological cycle, of which water vapour is a very important component, is still not properly represented in the current models (see http://www.ecmwf.int/research/era/Performance).

This difficulty in adequately measuring and modelling water vapour gives rise in part to the uncertainty mentioned above in the temperature increase estimates. The transport of water vapour, its sources and sinks through evaporation and precipitation, remain poorly quantified because the climatology and atmospheric processes have not been observed with the accuracy, precision, and coverage needed to understand them. In

particular, only sparse and inaccurate humidity data are available in the upper troposphere and tropopause region.

Climate models must be carefully validated before their predictions can be trusted. Accurately measured and model-independent consistent climatologies of temperature and water vapour will be essential means for validation. In this context, it is important that climate models are validated not only with respect to the observed mean climate, but also in their variability and against known external forcings (like volcanic eruptions) during the mission period. A simple but important example is the annual solar cycle and the associated seasons. Another example is heating rates from release of latent heat in association with monsoons, which can be validated by invoking data assimilation methods. In such cases, the observed data must be assimilated into the relevant atmospheric model and the parameters varied in such a way that the forcing (mainly heating) errors are minimised in a global sense.

The technique of minimizing forcing errors by assimilation of high quality analyses is already used in a range of European projects. However, a major obstacle when using data from currently available sources, such as radiosondes and vertical profiling from present satellites, is either their coarse spatial and temporal resolution and/or lack of sufficient accuracy and/or long-term stability and vertical coverage.

In particular, added to standard state parameter estimation, the technique of forcing error estimation can provide valuable guidelines for the construction of new and improved physical parameterisation algorithms (e.g. in radiation and cloud modelling).

The current operational systems of satellite sounding radiometers (passive infrared and microwave) provide information on tropospheric and stratospheric temperature and on tropospheric humidity with global coverage at high horizontal resolution. But the systems are deficient in vertical resolution since individual spectral channels have weighting functions of width 5-10 km. So the combined vertical resolution of the system is only 2-3 km in cloud-free areas and worse in cloudy areas, with humidity accuracies of about 20%. Future operational microwave sounders will have similar performance.

Externally forced climate variations are often split into terms related to natural and anthropogenic causes. Due to the high accuracy of the retrieved climate data, the basic monitoring of climate variations during the mission period is relatively straightforward using modern data assimilation techniques. However, it is a much more complicated problem to isolate those variations due to external forcings from those internal to the climate system. For example, the well-known El Niño/Southern Oscillation (ENSO) phenomenon gives rise to considerable variations in the global mean troposphere temperature. Other internal climatic variability mechanisms impact the total system in a similar manner. Thus a simple global mean temperature trend during the mission period will not tell us directly whether, for example, the greenhouse effect is increasing.

But by assimilating the observed occultation data into the atmospheric component of a climate model, it is possible to monitor variations in the models fitted to the observations and thereby obtain and identify 'fingerprints' of external forcings of the climate.

Another way of exploiting the ACE+ observations for climate change monitoring is to focus on the atmosphere mass field as represented in the information of the ACE+ global refractivity fields (Yuan et al. 1993). This more direct use of the observables requires no derivation of the standard meteorological parameters such as pressure, temperature, and humidity. Vedel and Stendel (2004) showed that the heights of refractivity surface fields are sensitive to climate change, and in stratosphere regions give an even more precise measure of global climate variations than presently known methods (Fig. 2.4). Furthermore, differential seasonal warmings can be detected from the refractivity fields once has a longer term database. Their climate data originated from simulations for a future climate evolution of a coupled atmosphere-ocean general circulation model (AOGCM) and the atmosphere climate model ECHAM4.

Calculations of climate warming indicate that the amount of water vapour in the atmosphere may increase by as much as 5% over the next 20 years. Model experiments show that excluding the effect of water vapour in the long-wave radiation calculations (Hall and Manabe 1999) reduces the global warming from 3.4 K to 1.1 K when doubling the atmosphere CO_2 content. Such an effect would mean a water vapour enhancement of more than a factor of three. Thus such indications of climate changes call for a mission like ACE+ to enhance and substantiate the observational database for the predictions.

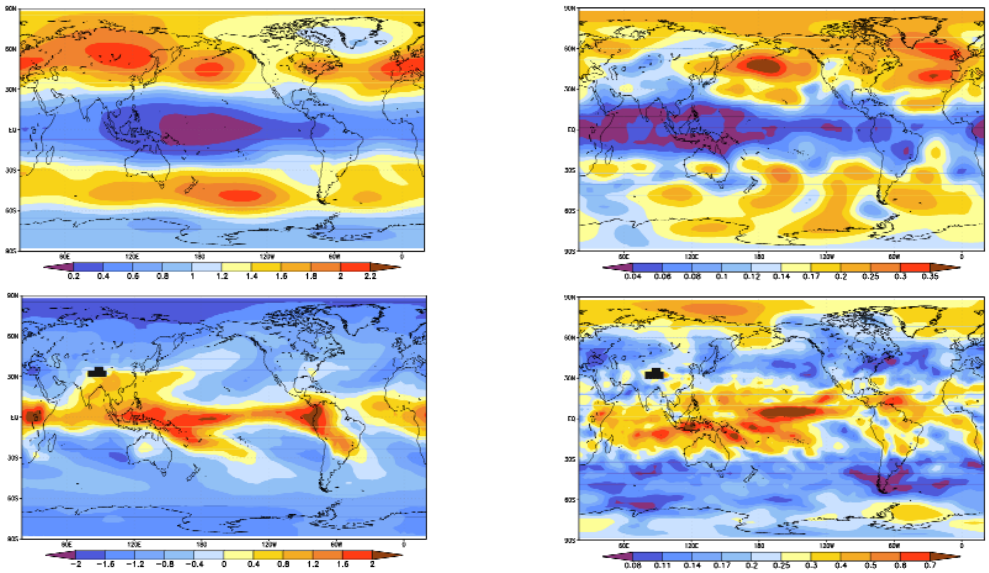

Figure 2.4: *The left panels give the climate induced global refractivity variations at two altitudes. The upper left panel is for the height of 15 km, while the lower left one is for 5 km. The right panels show the inter-annual variations of refractivity for the same altitudes (Vedel and Stendel 2004).*

2.3 Weather Prediction

ACE+ is a climate research mission and its mission requirements are driven by climate research objectives. Nevertheless, the nature of ACE+ observations also significantly benefits numerical weather prediction (NWP). The ACE+ mission will provide the database necessary for assessing the impact of GNSS-LEO and LEO-LEO-LEO data on NWP. A prototype retrieval chain for the observations has been implemented in a few European weather forecast centres, consisting of an observation processing system and 3D-Var assimilation. Refractivity as a function of geopotential height has been used in the model observation operators. The codes have been tested in impact trials assimilating CHAMP refractivity profiles. The control run was defined close to the operational set-up, assimilating radiosondes, ATOVS, SSMI, etc., but without radio occultation data. The impact trial run was defined identical to the control run except that now the CHAMP data were included. NWP forecast skill parameters were used to assess the results of the impact trial. Positive impact in forecast skill has been found already from the assimilation of ~160 occultation events per day (S.B. Healy, Met Office, UK, pers. comm. 2003).

2.4 Mission Timeliness

The ACE+ mission will provide high-quality data sets of tropospheric and stratospheric temperature and pressure measured simultaneously with tropospheric and lower stratospheric humidity with high vertical resolution. The consistent and simultaneous measurement of high-quality and high-resolution humidity and temperature profiles in this altitude range is new and unique. No other previous or presently planned satellite mission provides this type of atmospheric measurement, despite the urgent need for the product.

L-band (GPS) occultations have been successfully performed by several satellite instruments and will be continued by future instruments, in particular by MetOp and the COSMIC mission. COSMIC consists of a constellation of GPS-occultation satellites, similar to ACE+, but without using the GALILEO signal and, more importantly, without the X/K-band atmospheric absorption measurements. Furthermore, there would be little overlap in time with the COSMIC mission since the ACE+ launch will not take place before 2008, when COSMIC will already be close to the end of its lifetime. No other follow-on GPS occultation constellations are currently planned.

2.5 Heritage

Satellite-based GPS occultation techniques have a successful international heritage from past and present missions, including GPS/MET, SAC-C and CHAMP. ESA is also providing the L-band radio occultation instrument GRAS for the ESA/EUMETSAT MetOp mission, which is similar to the L-band receivers foreseen for ACE+.

The X/K-band satellite-satellite occultation technique is a novel concept without any predecessor. It would provide measurements of the atmospheric real and imaginary refractivity, while L-band occultation provides only the real refractivity.

2.6 Unique Contributions due to Unique Characteristics

The ACE+ mission can provide unique contributions thanks mainly to the following characteristics:

- High absolute accuracy and long-term stability of humidity, temperature, and pressure data due to intrinsic self-calibration of occultation data, which are Doppler shift (time standard) and transmission (normalised intensity) data.
- Rigorous independent measurement of humidity, temperature, and pressure vertical profiles in the free troposphere by the X/K-band occultations.
- High vertical resolution of fine structures in the atmosphere.
- All-weather capability due to the long probing wavelengths (>1 cm).
- Global and even coverage over both oceans and land.
- Radio occultation data can be used as reference data and do not need to be inter-calibrated with follow-on and non-overlapping radio occultation missions.

3. Research Objectives

ACE+ will contribute significantly to Science Themes 2 (Physical Climate) and 4 (Atmosphere and Marine Environment) of ESA's Living Planet Programme.

The **primary scientific objectives** of ACE+ are:

- Measure climate variability and trends as an initial key component of long-term occultation observations. The measurements can be made with high accuracy and more homogenously than existing observations, which is essential from a climate monitoring point of view. As a consequence, it is possible to compare data sets separated by many years and taken by different radio occultation sensors.
- Contribution to detection of climate changes and support of climate change predictions via provision of high-quality global reference data.
- Validation of Global Circulation Models (GCMs), both in terms of simulated mean climate and variability.
- Improvement, via data assimilation methods, of physics parameterisations in GCMs, and of the detection of external forcing variations.
- Improvement of the understanding of climate feedbacks determining magnitude and characteristics of climate changes.
- Study of structures in the troposphere and tropopause regions at high vertical resolution, in the context of atmospheric process research.
- Demonstration of the novel LEO-LEO occultation technique.
- Demonstration of the novel use of GALILEO-LEO occultation.

The ACE+ mission is primarily driven by climate research, with applications to weather, whereas conventional water vapour sounders are weather instruments with applications to climate.

The climate objectives will be achieved by measuring, analysing, and interpreting variations and changes in the global atmospheric humidity, temperature, and pressure (or geopotential height) distribution, in order to understand the current state and further evolution of the climate. In the upper troposphere in particular, ACE+ will be able to provide the climatology of water vapour with unprecedented accuracy, on global scales, with high vertical resolution (0.5-1 km), and long-term stability.

ACE+ will significantly improve our understanding of the climate system of the Earth. The water vapour and temperature data obtained by the LEO-LEO and GNSS-LEO radio occultation technique have several advantages compared to existing techniques. In the field of climate model validation and improvement, advanced data assimilation concepts, including parameter and sensitivity estimation methods far beyond state estimation, will play a key role. Due to their high absolute accuracy, ACE+

measurements can improve data assimilation bias correction schemes. The atmospheric physics studies on troposphere and tropopause structures will specifically exploit the high vertical resolution and accuracy of ACE+ occultation data.

ACE+ offers a key complement to the planned nadir-sounding high spectral resolution infrared instruments (AIRS, IASI, CrIS) in that clouds can be observed and their liquid water content can be estimated and corrected for. It also offers a fundamentally different alternative to the traditional sounding techniques, thus providing an invaluable tool for inter-validation of humidity, temperature and pressure (geopotential height).

The utility and performance of GALILEO-LEO occultation data will be thoroughly assessed, including assessment of the complementarity and potential performance advantages compared to the GPS-LEO occultations.

Indicating the versatile utility of ACE+ data, the mission can help advance our understanding of many important atmospheric physics and climate change processes by addressing such issues as:

- Global climate warming and related changes in atmospheric water vapour levels.
- Tropical heat and mass exchange with extra-tropical regions.
- Transport across subtropical mixing barriers, relevant for information on the lifetime of greenhouse gases.
- Stratospheric temperatures and atmospheric wave phenomena.
- Stratospheric temperature trends.
- Polar front dynamics and mass exchange together with tropospheric water vapour feedback on climate stability.
- High latitude tropospheric-stratospheric exchange processes related to polar vortex conditions.
- Climatology of Rossby waves and atmospheric internal waves.

Secondary scientific objectives of ACE+ are

- Contribution to improved numerical weather prediction (NWP).
- Support of analysis, validation and calibration of data from other space missions.

ACE+ data will provide a highly accurate humidity and temperature data set, with particular strength in the upper troposphere, which can be used in data assimilation systems and will therefore also benefit NWP models. In the reverse direction, advances in NWP will benefit climate studies, because the atmospheric analyses, a routine by-product of NWP systems, are highly valuable also for climate purposes, in particular the re-analyses (consistent analysis sequences over decades). However, it has to be

noted that the ECMWF re-analysis ERA-40, as currently available, is not suitable for water vapour trend studies.

Mutual support in analysis, calibration and validation of concurrent space missions is an important objective. Also during the time of ACE+ a series of space missions, both European and non-European, can sensibly exploit this type of synergy. As one example, the close collaboration with the nominally slightly overlapping GPS-LEO occultation mission COSMIC (Constellation Observing System for Meteorology, Ionosphere, and Climate) will be of particular interest.

Secondary objectives are important add-on objectives, which will be pursued and accounted for with as much dedication as available resources permit, but are not mission drivers.

Spin-off benefits of ACE+ are:

- Ionospheric climate and weather and space weather investigations.
- Assessment and improvement of present water vapour attenuation models.
- Turbulence products in the lower troposphere.

Ionosphere and space weather investigations comprise a wide range of specific objectives from electron density monitoring and modelling, via ionospheric and space weather prediction and data assimilation advancements, to studies of such phenomena and processes as ionospheric storms, travelling disturbances, current systems, and irregularities and scintillations. The electron density data provided by ACE+ for these purposes will be unique in their space/time coverage and vertical resolution.

Improved water vapour attenuation coefficients are important pieces of fundamental spectroscopic information. The ACE+ mission can potentially contribute via its LEO-LEO attenuation measurements near the centre and along the wing of the 22 GHz water vapour line. These data, complemented by accurate water vapour validation data (e.g. from water vapour lidar campaigns), should allow the derivation of more accurate spectroscopic coefficients, including an improved knowledge of their temperature dependence.

Radio scattering by refractivity inhomogeneities caused by atmospheric turbulence can result in scintillation phenomena in ACE+ data in the troposphere. Estimates of height variations of the scintillation power spectrum and of the refractive structure parameter may be possible, which can be interpreted in terms of power spectrum and variance of refractive index fluctuations. Details of the atmospheric turbulence such as its intermittency and the role of coherent structures can be studied. Of particular value for climate science, e.g. for improvement of turbulence parameterizations in climate models, will be global climatologies of kinetic energy dissipation rates, which can be deduced as well. Scientific information can furthermore be gained by joint analysis of

ACE+ scintillation parameters and profile measurements with ground-based meteorological data. Also due to the hazardous effect of turbulence on aircraft operations, its global monitoring via ACE+ could be of interest.

Spin-off benefits are not mission objectives, but additional ‘free’ benefits resulting from the mission design towards the scientific objectives summarized above. The spin-off benefits will be exploited on a best-effort basis.

4. Observation Requirements and Measurement Principle

Climate research in particular needs high-quality climate products with high vertical resolution, global coverage and high spatial and temporal sampling density. This section discusses the observational requirements that form the basis for the ACE+ mission concept. It also introduces the occultation measurement principle of ACE+.

In the Second Report on the Adequacy of the Global Climate Observing Systems [GCOS 2003], the generic requirements for observations in general are given. Special emphasis has been put on the usage of satellite data. Temperature and water vapour are named as essential upper-air climate variables. For effective climate monitoring systems, observations of the essential climate variables should adhere to the following general principles (in italics, excerpts only):

- *The exploitation of promising new techniques, including occultation techniques and ground-GPS-based water vapour sensing, is explicitly recommended.*
- *The impact of new systems or changes to existing systems should be assessed prior to implementation.* This has been done for the generic radio occultation (RO) technique by the experiments GPS/MET and CHAMP.
- *A suitable period of overlap for new and old observing systems should be required.* Due to the self-calibrating nature of the RO technique, this is not necessary, and is therefore a unique feature of this type of observation.
- *Satellite systems for monitoring climate need to be stable in the long-term with respect to calibration issues.* The RO technique embraces the concept of self-calibration (see also Chapter 5).

In addition, for satellite based systems:

- *A suitable period of overlap for new and old satellite systems should be ensured for a period adequate to determine inter-satellite biases and maintain the homogeneity and consistency of time-series observations.* For RO, this is not necessary due to the characteristics of the observation technique, as stated above.
- *Continuity of satellite measurements (i.e. elimination of gaps in the long-term record) through appropriate launch and orbital strategies should be ensured.*
- *Operational production of priority climate products should be sustained, and peer-reviewed new products should be introduced as appropriate.*
- *Data systems needed to facilitate user access to climate products, metadata and raw data, including key data for delayed-mode analysis, should be established and maintained.* This is part of the envisaged implementation.

In response to the climate mission objectives, ACE+ will collect atmospheric profiles of humidity and temperature (and pressure/geopotential height) as a function of height

with the high accuracy and vertical resolution needed for the establishment of global climatologies of tropospheric humidity and tropospheric and stratospheric temperature. Atmospheric refractivities will be retrieved, amongst other data, as an intermediate product (see Chapter 5) with its own scientific value (see Chapter 2).

4.1 Generic Observational Requirements

Table 4.1 summarises the observational requirements for climate applications, i.e. uses such as climate monitoring, analyses, and prediction (WMO 1996, 2000a, 2000b). These requirements are generic, and independent of any particular observing system. Following WMO definitions, the requirements are broken down into atmospheric layers as follows:

Lower troposphere	LT	1000 hPa – 500 hPa	approx. surface – 5 km
Higher troposphere	HT	500 hPa – 100 hPa	approx. 5 km – 15 km
Lower stratosphere	LS	100 hPa – 10 hPa	approx. 15 km – 35 km
Higher stratosphere	HS	10 hPa – 1 hPa	approx. 35 km – 50 km

		Specific Humidity	Temperature
Horizontal Domain		Global	Global
Horizontal Sampling	**LT**	50-100 km	50-500 km
	HT	50-100 km	50-500 km
	LS	50-250 km	50-500 km
	HS	50-250 km	50-500 km
Vertical Domain		Surface to 1 hPa	Surface to 1 hPa
Vertical Sampling	**LT**	0.5-2 km	0.3-3 km
	HT	0.5-2 km	1-3 km
	LS	0.5-2 km	1-3 km
	HS	1-3 km	5-10 km
Time Domain		> 10 years	> 10 years
Time Sampling		3-12 hrs	3-12 hrs
RMS Accuraacy (1)	**LT**	0.25-1 g/kg	0.5-3 K
	HT	0.025-0.1 g/kg	0.5-3 K
	LS	0.0025-0.01 g/kg	0.5-3 K
	HS	0.00025-0.001 g/kg	1-3 K
Long-term Stability		< 2% RH(2)/decade	< 0.1 K/decade
Timeliness	**Climate**	30-60 days	30-60 days
	NWP	1-3 hrs	1-3 hrs

(1) understood to be the accuracy at a vertical resolution consistent with the required sampling (i.e. a resolution of 2 × Vertical Sampling [km]).

(2) stability is specified for Relative Humidity (RH) here, a quantity with well-defined and linear range over the vertical domain. There are standard methods to convert between RH and specific humidity as functions of temperature and pressure.

Table 4.1: *Generic observational requirements for climate applications.*

Related to data assimilation, it is noted that for standard climate model runs observational data are not assimilated directly. Instead, pre-analysed fields are used for forcing and validation. Since these fields often come from operational NWP analyses, a generic NWP timeliness specification is also included in Table 4.1. Re-analyses data sets would be optimal for use in climate models, but since re-analyses are not performed regularly, operational (NWP) analyses are used instead.

4.2 Measurement Principle of ACE+

4.2.1 LEO-LEO Occultations

The core part of ACE+ is the novel X/K-band cross-link occultation (LEO-LEO occultation) between pairs of counter-rotating ACE+ satellites measuring the atmospheric refractivity and absorption. ACE+ will actively sound the atmosphere using LEO-LEO signal transmission at three frequencies around the 22 GHz water vapour absorption line (nominally placed near 10, 17, and 23 GHz). Measurements of the occulted phase and amplitude of the electric field from the LEO transmitter at these frequencies will deliver independent information on both humidity and temperature profiles, which will lead to atmosphere data of unprecedented accuracy.

Figure 4.1 depicts the ACE+ observational geometry. In order to realise global coverage and the LEO-LEO satellite cross-link, at least two satellites need to fly counter-rotating in high-inclination orbits. In order to ensure adequate coverage to achieve all primary scientific objectives, a total of four satellites has to be placed into the two orbits (two satellites in each orbit; two pairs of LEO-LEO transmitter and receiver).

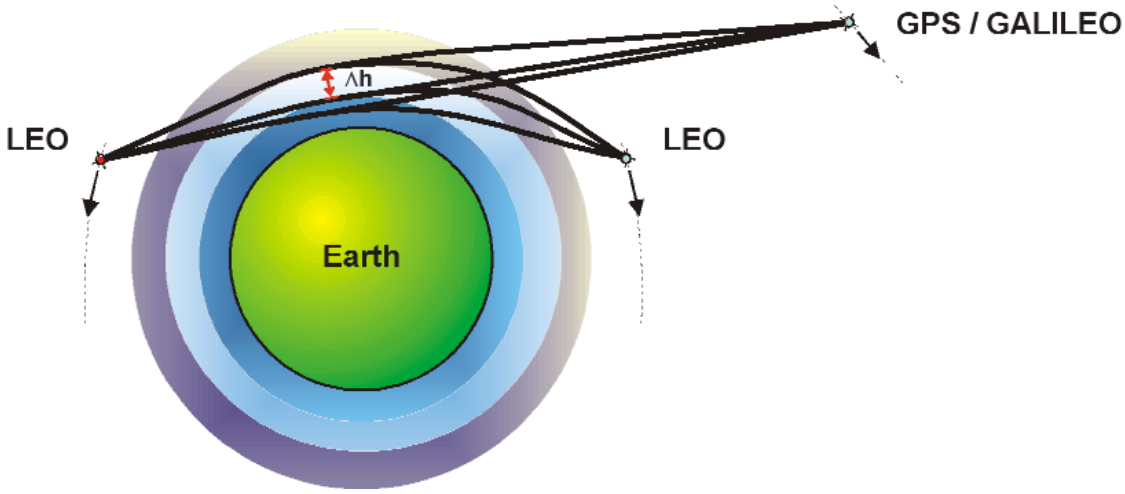

Figure 4.1: *Schematic of the observation geometry for LEO-LEO and GPS/GALILEO-LEO occultation (Source: Danish Meteorol. Institute).*

The baseline is four satellites in two counter-rotating Sun-synchronous orbits. These orbits should be aligned in the local time of the orbit nodes (equator crossings) with the orbit of the European MetOp satellite series for synergy reasons. A higher orbit (possibly near 800 km) should contain two satellites, while the counter-rotating lower orbit (possibly near 650 km) should contain the other two satellites. Whenever an ACE+ receiver satellite meets over limb an ACE+ transmitter satellite of the other orbit, a rising or setting X/K-band occultation event between the two satellites will occur.

During a LEO-LEO occultation, both the amplitude and phase of the coherent signal will be measured at three different frequencies. Water vapour absorption as function of frequency is not symmetric around the 22 GHz absorption line, and also liquid water contributes to absorption. Utilizing three frequencies can essentially remove the effect of liquid water droplets in clouds from the process of estimating the profiles of tropospheric humidity and temperature. The atmospheric absorption in the relevant frequency range is illustrated in Figure 4.2.

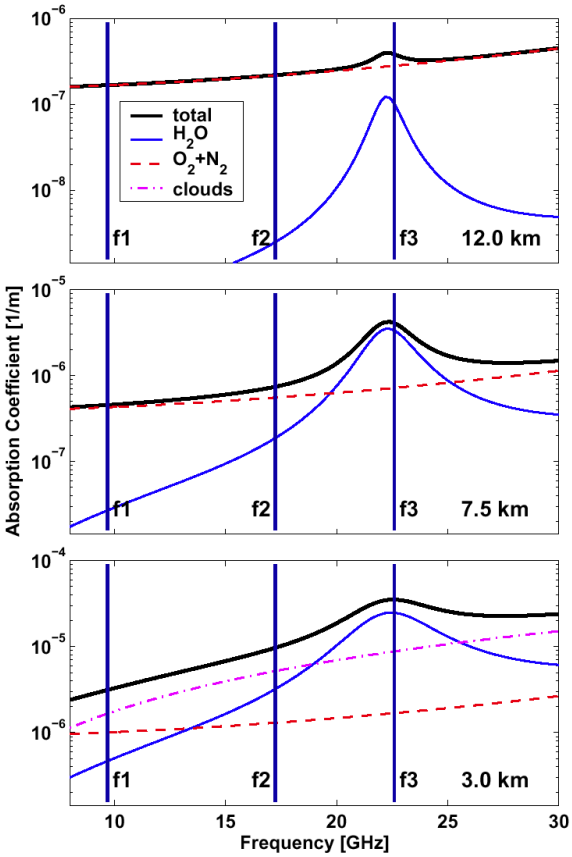

Figure 4.2: *Atmospheric absorption coefficients as a function of frequency at three different heights (3 km, 7.5 km, 12 km) for a mid-latitude summer atmosphere. The three ACE+ baseline frequencies are indicated. In addition to total absorption, water vapour (H_2O), ambient air (O_2), and liquid water (cloud; lowest panel) absorption are also shown (Source: Chalmers Univ. of Technology).*

The transmitted coded X/K-band signals, with similar signal structure as the GPS signals, are key observables for monitoring the global distribution of atmospheric water vapour in the future. The microwave cross-links must be engineered to handle the expected water vapour absorption, while delivering the required measurement precision. In the troposphere below about 6 km, where water vapour is fairly abundant, one uses the less strongly absorbed 10 and 17 GHz signals, which will allow accurate measurements down to approximately the top of the atmospheric boundary layer. In the upper troposphere, where the moisture concentration can be orders of magnitude lower than in the lower troposphere, the overriding consideration is detecting the relatively weak effect with sufficient precision in order to achieve accurate moisture measurements. Another frequency near 23 GHz, close to the 22.235 GHz absorption line centre, is therefore essential to cover this height range.

4.2.2 GNSS-LEO Occultations

The GNSS radio occultation method uses limb sounding to retrieve the parameters of the neutral atmosphere in the stratosphere and the troposphere. It can also sense electron density in the ionosphere. The basis of the radio occultation technique relies on the fact that the radio waves of the satellite navigation system (GPS or GALILEO) get refracted along the ray path of the wave, by an amount determined by the dispersion of the media, as they pass through the atmosphere (either during a rise event or a setting event as seen from the receiver). The refractivity profile can then be derived from the observation of phase change and amplitude variations.

In the stratosphere and the upper troposphere, where the humidity is low, refraction is dominated by vertical temperature gradients, and the temperature profile can be retrieved accurately. In the lower troposphere, where humidity effects play the major role, water vapour profiles can be retrieved even allowing for typical uncertainties in the prior knowledge of temperature. In the tropics, the typical border between the two regimes is at an altitude of ~7-8 km, while in the dry polar atmosphere accurate temperature sounding is possible down to the atmospheric boundary layer.

4.3 ACE+ Mission-Specific Observational Requirements

The generic requirements for climate research given in Table 4.1 have been refined in order to address the specific scientific mission objectives of ACE+. This section summarises the scientific requirements. The two elements of the mission are the X/K-band LEO-LEO occultations and the L-band GNSS-LEO occultations.

The LEO-LEO observations provide the novel, highly accurate and independent measurement of humidity and temperature profiles and are the primary component of ACE+. The GNSS-LEO observations support the scientific requirements through the vast amount of atmospheric refractivity measurements from which temperature and

humidity can be retrieved, involving a priori information in the troposphere (e.g. via 1D-Var retrieval).

The observational requirements are expressed as *target requirements* defining the desired product performance and *threshold requirements* defining the minimum required performance necessary to achieve the scientific mission goals.

The ACE+ mission-specific requirements are given in Table 4.2 for the LEO-LEO observations, and in Table 4.3 for the GNSS-LEO observations. They are based on specifications of climate research groups as well as NWP centres. Climate research is currently changing its focus on higher resolution, as evidenced by the increasing number of global high-resolution simulations and regional climate studies. This research is based on observations and modelling with horizontal resolutions of 100-200 km for global simulations and 20-50 km for regional simulations. Vertical resolutions of several hundred meters are used up to 3 km. These resolution definitions are the proposed baselines for the Fourth Assessment Report of the IPCC, to be completed in 2007.

The overall RMS accuracy level is guided by the requirements of NWP centres. This is based on the fact that instruments with an error larger than the NWP requirements can be replaced by already existing instruments. It must be taken into account that the errors for some observation regions may not coincide with climate research and NWP interests.

		Specific Humidity		Temperature	
		Target	Threshold	Target	Threshold
Horizontal domain		global			
Horizontal sampling (mean distance of adjacent profiles) *to be achieved within:* time sampling		700 km	1600 km	700 km	1600 km
		24 hrs			
No. of profiles per grid box[1] per month		40	30	40	30
Vertical domain[2]		TBL[3] to 15 km	5 to 12 km	TBL[3] to 50 km	5 to 40 km
Vertical sampling	LT	0.5 km	1 km	0.5 km	1 km
	HT	0.5 km	1 km	0.5 km	1 km
	LS	-	-	0.5 km	1 km
	HS	-	-	1 km	5 km
RMS accuracy[4]	LT-*TBL*	0.6 g/kg	1 g/kg	1 K	2 K
	LT-*top*	0.2 g/kg	0.4 g/kg	1 K	2 K
	HT-*top*	0.003 g/kg	0.025 g/kg	0.5 K	1 K
	LS	-	-	0.5 K	1 K
	HS	-	-	1.5 K	3 K
Long-term stability		2% RH[5] per decade	3% RH[5] per decade	0.1 K per decade	0.15 K per decade
Timeliness	climate	30 days	60 days	30 days	60 days
	NWP[6]	1.5 hrs	3 hrs	1.5 hrs	3 hrs
Time domain[7]		5 years			

[1] Grid box defined as square of horizontal sampling requirement (box of size 'horiz. sampling' [km] x 'horiz. sampling' [km])

[2] Below about 3 km (typical atmospheric conditions) to 6 km (severe scintillation/cloudiness conditions), retrievals may involve weak prior temperature information (e.g. extrapolation from above the top height of such conditions into the lower troposphere) to separately derive humidity and temperature from refractivity/absorption; above, humidity, temperature, and pressure shall be derived as function of height without such prior information.

[3] Top of atmospheric boundary layer, located typically 1-2.5 km above the surface. Below Max{TBL, 2 km}, retrievals shall be performed on a best-effort basis.

[4] Understood to be the accuracy at a vertical resolution consistent with the required sampling (i.e. a resolution of 2 × Vertical Sampling [km]). The humidity accuracy requirement shall be understood to decrease linearly between the specified values at LT-*TBL*=2 km and LT-*top*=5 km and to decrease logarithmically, as ln(humidity), from LT-*top*=5 km until it reaches the specified HT-*top* value at 10 km; above, the height dependence shall be constant. The temperature accuracy requirement shall be understood constant between the specified values at LT-*TBL*=2 km and LT-*top*=5 km and to decrease linearly from LT-*top*=5 km until it reaches the HT-*top* value at 10 km; above, the height dependence shall be constant.

[5] Stability is specified for Relative Humidity (RH) here, a quantity with well-defined and linear range over the vertical domain. There are standard formulae to convert between RH and specific humidity as functions of temperature and pressure.

[6] NWP is secondary mission objective. However, often NWP analyses are used for the forcing of climate GCM runs. Therefore, the climate mission objectives would benefit if this timeliness requirement would be fulfilled.

[7] Climate change detection and monitoring requires long-term observations over decades. ACE+ should thus be followed by similar missions. The ACE+ mission objectives, however, can be fulfilled within the given time frame.

Table 4.2: *LEO-LEO observational requirements.*

		Specific Humidity		Temperature	
		Target	Threshold	Target	Threshold
Horizontal domain		global			
Horizontal sampling (mean distance of adjacent profiles) *to be achieved within:* time sampling		100 km	700 km	100 km	700 km
		12 hrs			
No. of profiles per grid box[1] per month		50	40	50	40
Vertical domain[2]		TBL[3] to 10 km	2.5 to 5 km	TBL[3] to 50 km	5 to 40 km
Vertical sampling	LT	0.5 km	1 km	0.5 km	1 km
	HT	0.5 km	1 km	0.5 km	1 km
	LS	-	-	0.5 km	1 km
	HS	-	-	1 km	5 km
RMS accuracy[4]	LT-*TBL*	0.6 g/kg	1 g/kg	1 K	2 K
	LT-*top*	0.2 g/kg	0.4 g/kg	1 K	2 K
	HT-*10 km*	0.1 g/kg	0.2 g/kg	0.5 K	1 K
	LS	-	-	0.5 K	1 K
	HS	-	-	1.5 K	3 K
Long-term stability		2% RH[5] per decade	3% RH[5] per decade	0.1 K per decade	0.15 K per decade
Timeliness	climate	30 days	60 days	30 days	60 days
	NWP[6]	1.5 hrs	3 hrs	1.5 hrs	3 hrs
Time domain[7]		5 years			

(1) Grid box defined as square of horizontal sampling requirement (box of size 'horiz. sampling' [km] × 'horiz. sampling' [km])

(2) Below about 5 km (dry conditions) to 12 km (moist tropical conditions), retrievals will involve prior information to separately derive humidity and temperature from refractivity; above, humidity sensitivity is negligible and temperature and pressure shall be derived as function of height without such prior information.

(3) Top of atmospheric boundary layer, located typically 1-2.5 km above the surface. Below Max{TBL, 2 km}, retrievals shall be performed on a best-effort basis.

(4) Understood to be the accuracy at a vertical resolution consistent with the required sampling (i.e. a resolution of 2 × Vertical Sampling [km]). The humidity accuracy requirement shall be understood to decrease linearly between the specified values at LT-*TBL*=2 km and LT-*top*=5 km and to decrease logarithmically, as ln(humidity), from LT-*top*=5 km until it reaches the specified HT-*top* value at 10 km; above, the height dependence shall be constant. The temperature accuracy requirement shall be understood constant between the specified values at LT-*TBL*=2 km and LT-*top*=5 km and to decrease linearly from LT-*top*=5 km until it reaches the HT-*top* value at 10 km; above, the height dependence shall be constant.

(5) Stability is specified for Relative Humidity (RH) here, a quantity with well-defined and linear range over the vertical domain. There are standard formulae to convert between RH and specific humidity as functions of temperature and pressure.

(6) NWP is secondary mission objective. However, often NWP analyses are used for the forcing of climate GCM runs. Therefore, the climate mission objectives would benefit if this timeliness requirement would be fulfilled.

(7) Climate change detection and monitoring requires long-term observations over decades. ACE+ should thus be followed by similar missions. The ACE+ mission objectives, however, can be fulfilled within the given time frame.

Table 4.3: *GNSS-LEO observational requirements.*

5. Data Processing Requirements

This chapter discusses the data processing requirements, particularly with respect to Level 2. Level 1-to-Level 2 processing ('Level 2 processing' hereafter) requires conversion of bending angles (GNSS-LEO) or bending angles and transmissions (LEO-LEO) into atmospheric variables. The main ACE+ sounding products anticipated at Level 1b and Level 2 are summarized in Table 5.1.

Level	GNSS-LEO	LEO-LEO
Level 1b	• Doppler shift and raw transmission (1) profiles (at L1+L2) vs. time • Bending angle profiles vs. impact parameter	• Doppler shift and raw transmission (1) profiles (at 3 frequencies) vs. time • Bending angle profiles vs. impact parameter • Transmission profiles (at 3 freq.) vs. time
Level 2	• Real refractivity profiles vs. height	• Real refractivity profiles vs. height • Imaginary refractivity profiles (at 3 frequencies) vs. height
	• Humidity profiles vs. height • Temperature profiles vs. height • Pressure and geopotential height profiles vs. height • Error estimates and meta-data for all retrieved Level 1b & Level 2 profiles	

(1) 'Raw transmission' is the normalized received power ($P(t)/P_{above\text{-}atmos}$) including defocusing and absorption, whilst the 'Transmission' includes absorption only (*Transmission* = 1 – *Absorption*).

Table 5.1: *Main ACE+ Level 1b and Level 2 data products.*

The product domain will be global, and from 2 km to 50 km in height. All Level 2 products will be available to users within 30 days of observation time, and a significant fraction of the data also in near-real time for NWP use on best-effort basis. The performance requirements on the Level 2 data products have been summarized in Chapter 4.

Level 2 processing implies the application of retrieval techniques to derive geophysical quantities from the Level 1a/b data. In all cases, care has to be taken regarding precise knowledge of the error characteristics. Quality checks need to be performed at all levels. Below, the established GNSS-LEO processing is briefly treated first, followed by the LEO-LEO processing. Processing by data assimilation techniques is also addressed. Space constraints allow only a limited discussion here; for a more extended summary on the ACE+ data processing see Kirchengast et al. (2004b).

5.1 GNSS-LEO Processing

The Level 2 processing of GNSS-LEO data was developed in the framework of other occultation missions such as GPS/MET, CHAMP/GPS, and MetOp/GRAS, and is now

fairly mature (e.g., Melbourne et al. 1994, Hoeg et al. 1995, Kursinski et al. 1997, Syndergaard 1999, Steiner et al. 1999, Healy and Eyre 2000, Rieder and Kirchengast 2001, Steiner et al. 2001, Hajj et al. 2002).

The GNSS-LEO Level 2 processing is a well-posed essentially linear (except in the lower troposphere) retrieval problem involving simple fundamental equations only such as an Abelian Transform (Fjeldbo et al. 1971), the real refractivity equation (Smith and Weintraub 1953), the hydrostatic equation, and the equation of state. In the troposphere, separation of temperature and humidity from refractivity requires background (a priori) information, e.g. via 1D-Var retrieval (Healy and Eyre 2000). A detailed algorithmic description can be found in Kirchengast et al. (2004a) and the references cited above, among which the reviews by Kursinski et al. (1997), Syndergaard (1999), and Steiner et al. (2001) are particularly instructive.

The main areas where further GNSS-LEO algorithm advancements are being worked on include wave-optics-based processing in the lower troposphere (e.g. Gorbunov 2002, Jensen et al. 2003), improved retrievals in the upper stratosphere (e.g. Gobiet et al. 2004), improved error characterization (e.g. Marquardt and Healy 2003, Steiner and Kirchengast 2004), and open-loop tracking data processing (e.g. Sokolovskiy 2001). The processing of open-loop data merits particular attention in the future. While so far no real instrument data of this type exist, the data from MetOp/GRAS, the first instrument with adequate capabilities in terms of SNR and fully-fledged open-loop measurement mode, will certainly spur on these activities.

5.2 LEO-LEO Processing

The scientific processing of LEO-LEO occultation data starts from phase and amplitude data, supplemented by the necessary geometric information, and proceeds via Doppler shifts, bending angles, and transmissions down to quasi-vertical atmospheric profiles of real and imaginary refractivities, density, pressure, geopotential height, temperature, humidity, and liquid water. The algorithms consist of the following main steps:

1. bending angle and transmission retrieval (part of Level 1b processing),
2. real and imaginary refractivity retrieval,
3. atmospheric profile retrieval.

Bending angle, transmission and refractivity retrievals proceed similar to the GNSS-LEO case and will be only briefly addressed below. The emphasis is placed on the description of a tentative atmospheric profiles retrieval processing scheme. More details can be found in Kirchengast et al. (2004a) and Nielsen et al. (2003), with complementary information also to be found, for example, in Kursinski et al. (2002). The processing chain was implemented in an end-to-end simulator to derive the performance results discussed in Chapter 6.

Figure 5.1 illustrates the LEO-LEO Level 2 processing schematically with particular emphasis on the atmospheric profile retrieval.

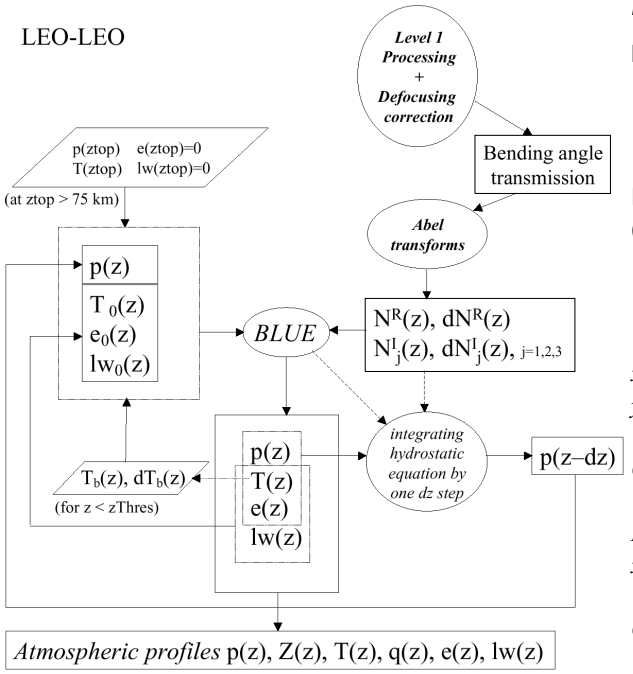

BLUE (Best Linear Unbiased Estimator):

Baseline case (z_{Thres} = 0):

$$\boldsymbol{x}_{n+1} = \boldsymbol{x}_n + \left(\boldsymbol{K}_n^T \cdot \boldsymbol{C}_y^{-1} \cdot \boldsymbol{K}_n\right)^{-1} \cdot \left[\boldsymbol{K}_n^T \boldsymbol{C}_y^{-1}\left(\boldsymbol{y} - \boldsymbol{y}_n^{\mathrm{mod}}(\boldsymbol{x}_n)\right)\right]$$

In case of severe turbulence for $z < z_{Thres}$ (z_{Thres} about 3 to 6 km):

$$\boldsymbol{x}_{n+1} = \boldsymbol{x}_n + \left(\boldsymbol{K}_n^T \cdot \boldsymbol{C}_y^{-1} \cdot \boldsymbol{K}_n + \boldsymbol{C}_b^{-1}\right)^{-1} \cdot \left[\boldsymbol{K}_n^T \boldsymbol{C}_y^{-1}\left(\boldsymbol{y} - \boldsymbol{y}_n^{\mathrm{mod}}(\boldsymbol{x}_n)\right) - \boldsymbol{C}_b^{-1}(\boldsymbol{x}_n - \boldsymbol{x}_b)\right]$$

x_n: state vector to be estimated

y_n, y_n^{mod}: measurement vector, forward-modeled measurement vector

C_y: measurement (and forward modeling) error cov. matrix

K_n: Jacobian weighting matrix

x_b: background (a priori) state vector

C_b: background (a priori) error covariance matrix

Figure 5.1: *Schematic of the LEO-LEO Level 2 processing.*

Bending Angle and Transmission Retrieval

The phase and amplitude profiles are used together with the corresponding precise orbit determination (POD) data comprising positions and velocities of LEO transmitter and LEO receiver satellites to determine the atmospheric bending angle profile as a function of impact parameter in the same way as in the well-known GNSS-LEO processing. If wave-optics processing is utilized, both phase path changes (Doppler shift profiles) and normalized amplitude profiles (raw transmission profiles) are used in this process, whereas if geometric-optics processing is performed only Doppler shift profiles are used. The Doppler shift data, which directly relate to the bending angle data, are the key data for the intrinsic self-calibration: each single Doppler shift profile, together with its associated precise orbital state profiles from POD, is an absolute measure of the height-dependent bending angle at the time and location of the event, independent of any auxiliary calibration data and of any other measurements before, in parallel, or after the ~30 sec duration of an occultation event.

The amplitude profiles at each LEO-LEO signal frequency (ACE+ nominal frequencies near 9.7 GHz, 17.25 GHz, 22.6 GHz), the impact parameter profile, and the transmitter and receiver position profiles are used to compute the transmission profiles due to atmospheric absorption at each frequency. The best way to subtract amplitude defocusing and spreading from the measured amplitude profiles, in order to obtain the

transmission profiles due to absorption only, depends on whether wave-optics or geometric-optics processing is utilized.

A key step in transmission retrieval is the normalization to a reference height 'above the absorptive atmosphere', where the transmission is unity (~25 km in the ACE+ case). This is the step where the intrinsic self-calibration of the amplitudes comes in: similar to the self-calibrated bending angles, this normalization implies that as long as the transmission measurements are stable in the short-term over the ~30 sec of the occultation event from about 25 km towards the surface, each individual profile is a self-standing reliable measure of the atmospheric absorption at the given place and time, independent of any other measurements. Moreover, since the imaginary refractivity (or absorption coefficient) obtained from the transmission depends on the impact parameter-derivative of transmission only, a small constant transmission residual does not matter.

Real and Imaginary Refractivity Retrieval

The bending angle profile as a function of the impact parameter is converted to the real refractivity profile as a function of height via the classical GNSS-LEO Abel transform. Based on this, the real refractivity profile and the impact parameter profile are used together with the transmission profiles at each LEO-LEO frequency to derive the imaginary refractivity profiles as a function of height with another Abel transform akin to the classical one (same Abelian integration kernel but different in integrand; Kursinski et al. 2002, Kirchengast et al. 2004a). Since imaginary refractivity is proportional to the absorption coefficient, the latter can be obtained alternatively or in addition.

If data assimilation of LEO-LEO data products is performed, the refractivity profiles obtained will be the Level 2 data products most conveniently used in such schemes, since both real and imaginary refractivities at any point in space and time are just local functions of the atmospheric parameters.

Atmospheric Profile Retrieval

The real and imaginary refractivity profiles are associated with four equations: three equations from the frequency dependent imaginary refractivity profiles (N^I_1, N^I_2, N^I_3) and one equation from the real part (N^R), because this is practically non-dispersive for the frequencies considered. While the equation for the real part is a simple formula (Smith and Weintraub 1953), the equations behind the imaginary refractivity as a function of the atmospheric parameters are more elaborate and embodied in a Millimetre-wave Propagation Model (MPM) (e.g. Liebe et al. 1993). Together with the hydrostatic equation and the equation of state, there is a set of six equations to derive the four desired atmospheric parameters: pressure, temperature, humidity and liquid water. The latter, cloud liquid water, is retrieved as a by-product since it can have a strong impact on the absorption signal and is an important parameter for both climate applications and meteorology.

Because the set of equations is somewhat over-determined, it is still possible to retrieve all desired parameters if one of the imaginary refractivity information pieces is lost, as will be the case at any given height level, where only two of the three frequencies provide amplitude data in a useful dynamic range. The information on real refractivity at the lowest of the transmitted frequencies will be lost only in extreme (and rare) situations. If the imaginary refractivity variances grow large enough in the lower troposphere to render the Best Linear Unbiased Estimation (BLUE) problem effectively underdetermined, which can happen in the case of atmospheric turbulence, the advanced processing described below will be used.

Processing in case of severe atmospheric turbulence

Strong amplitude scintillations due to atmospheric turbulence can introduce significant noise into the imaginary refractivity data and may degrade the above baseline retrieval of atmospheric profiles below about 3 to 6 km in the troposphere. However, since the parts of the signal affected by scintillation can be identified thanks to the high sampling rate of the raw measurements (1 kHz), this enables a constant monitoring of the high frequency fluctuations and the determination of a 'threshold height', z_{Thres}, below which the imaginary refractivity data should be used with caution and potentially receive low to negligible weight in the BLUE process. As turbulence is a layered phenomenon (e.g. Gage 1990), usually only some fraction of the height levels below z_{Thres} may need to receive such down-weighting. This will have to be confirmed in future studies. In the performance analyses of Chapter 6 it has been assumed, as a conservative limit, that the complete height range below any z_{Thres} found is filled with turbulence.

In case of down-weighting applied to imaginary refractivities below z_{Thres}, one sensible way to cure the consequent under-determination of the BLUE problem is to introduce weak background (*a priori*) information into the retrieval at the height levels concerned. The primary candidate information for this purpose is temperature, since it is well predictable in the troposphere above the boundary layer and since it is sufficient auxiliary information under all conditions to ensure a robust estimation. Suitable background temperature profiles (T_{b}) can be obtained from a profile search in an adequate database (e.g. from a 24h ECMWF forecast in a geographic area of some degrees around the profile co-located with the measurement). The T_{b} profile selected can be the one that best fits the retrieved temperature profile in the troposphere right above z_{Thres}, where the retrieved data are still very accurate and allow for a good fit. The fit to the retrieved data, and not just selection of a co-located profile, is to avoid importing any potential small bias from the background into the retrieval (though ECMWF temperatures below 8 km are essentially unbiased). In Chapter 6 this 'best-fit T extrapolation' approach has been used for heights below z_{Thres} and found to ensure accurate humidity and temperature retrieval also under severe turbulence conditions.

Future Work on LEO-LEO Scientific Algorithms

The preliminary algorithm described above already provides satisfactory results (see Chapter 6). In the future, algorithms for severe turbulence situations will have to be studied in more detail in order to ensure an optimal solution. Techniques such as wave-optics approaches (e.g. Full Spectrum Inversion; Jensen et al. 2003) can perhaps be used to reduce scintillation fluctuations already on the transmission measurements (Level 1b) so that less down-weighting of imaginary refractivity data will be required at the atmospheric profile retrieval step.

As the LEO-LEO component is the novel part of ACE+, future processing advancements are possible and required at all steps of the retrieval chain: From detailed performance analyses of different methods to derive transmission profiles (both geometric-optics and wave-optics based) to optimized atmospheric profiles retrieval (both without and with presence of turbulence), future developments shall ensure exploitation of the LEO-LEO data in the best possible manner.

5.3 Processing by Data Assimilation Techniques

The ACE+ measurements shall be extensively exploited via data assimilation schemes, both alone as climate benchmark data for such purposes as climate model validation, testing, and improvement as well as together with other upper air and surface observations for re-analysis purposes. The importance and various modes of employing data assimilation to ACE+ data have been described by ESA (2001), Hoeg and Kirchengast (2002), and Kirchengast and Hoeg (2004).

Basically, the observations can be assimilated at four different levels:

- assimilation of retrieved atmospheric parameters (e.g. humidity, temperature),
- assimilation of real and imaginary refractivities,
- assimilation of bending angle and transmission profiles,
- assimilation of Doppler shifts and raw transmission profiles.

The closer the data are to the atmospheric parameters used by the model, the simpler is the assimilation scheme. On the other hand, the more data processing is carried out on the measured signals, the more difficult it is to accurately specify the required observation error covariance matrices. Assimilation of real and imaginary refractivities, or of bending angle and transmissions, can be statistically optimal using variational techniques, now common in assimilating passive radiance data from satellites. The assimilation of real refractivity has been prepared already (e.g. Healy and Eyre 2000) and the assimilation of imaginary refractivities would only require the use of a different local refractivity formulation, which is available (an MPM model instead of the Smith-Weintraub formulation).

Assimilation of more raw products would require more complex observation operator formulations, but would not involve spherical symmetry assumptions. For example, operators can be constructed that account for horizontal variations through the iterative use of a ray-tracer (e.g. Zou et al. 1999). However, simpler operators are also available for refractivities, which properly account for horizontal variations and spherical asymmetries by modelling 'Abelian weighted' refractivity profiles (Syndergaard et al. 2004).

Future advances required in assimilation processing related to ACE+ will include in particular the development and optimization of techniques dedicated to the assimilation of imaginary refractivities and transmissions, as well as the detailed analysis and quantification of error covariance matrices for all retrieved Level 1b and Level 2 data products. In addition, beyond Level 2 processing, advances in climate data assimilation systems for the purposes of model validation, testing, and improvement will be required.

6. Performance Estimation

The scientific requirements established for ACE+ have been given in Chapter 4 for both LEO-LEO and GNSS-LEO occultation. The key atmospheric parameters, on which the ACE+ observational requirements have been defined there, are humidity and temperature. The performance estimation results are presented in this chapter.

LEO-LEO occultation is the new technique enabling accurate independent measurement of humidity and temperature as discussed in the previous chapters. The feasibility of the LEO-LEO observations and the compliance of the data product quality with the scientific requirements has been demonstrated and is presented in the first section below. The performance of the GNSS-LEO occultation has been proven extensively in the past, including with current satellite missions such as CHAMP. The GNSS-LEO performance is thus only briefly re-called below. Finally, the performance of the mission, for both LEO-LEO and GNSS-LEO, for quantifying climate variability and trends over the mission lifetime of 5 years is addressed.

An end-to-end simulator, including the LEO-LEO retrieval algorithms discussed in Chapter 5, has been used for the performance assessment. The simulator, EGOPS5 (End-to-end Generic Occultation Performance Simulator, Version 5), was developed as an advancement and extension of the established EGOPS4 simulator for GNSS-LEO occultation (Kirchengast et al. 2002).

Due to space constraints, only a limited selection of the results is shown here. For a more extended overview of ACE+ performance results, see Kirchengast et al. (2004a,b).

The technical concept description and evaluation can be found in the technical annex.

6.1 LEO-LEO Occultation Performance

Representative performance assessment scenarios based on both a climatological atmosphere and an ECMWF high-resolution analysis field are discussed. The instrumental errors for all scenarios (thermal noise, instrumental 1/f noise, amplitude drift errors) have been modelled according to the defined ACE+ system/instrument requirements. The LEO transmitter and receiver orbits have been assumed consistent with the Phase-A baseline (orbital heights near 650 km and 800 km, etc.). The vertical resolution of the retrieved profiles is ~1 km for all scenarios shown, in line with the respective target requirements (Chapter 4).

6.1.1 Climatological Atmosphere Cases

A large number of atmospheric scenarios were analysed based on the CIRA86aQ moist-air climatology model (Kirchengast et al. 1999), supplemented by a simple cloud model (Eriksson et al., ESA-ACEPASS study pers. comm. 2003), and an atmospheric

turbulence/scintillation model (Sterenborg and Poiares-Baptista, ESA/ESTEC, pers. comm. 2003). Five representative CIRA86aQ cases were defined for this purpose, which together cover humidity and temperature conditions from tropical summer to high-latitude winter. The respective humidity and temperature profiles are illustrated in Figure 6.1. The scenarios discussed here all use the mid-latitude summer case, results including the other cases are shown by Kirchengast et al. (2004a) and Gradinarsky et al. (2003).

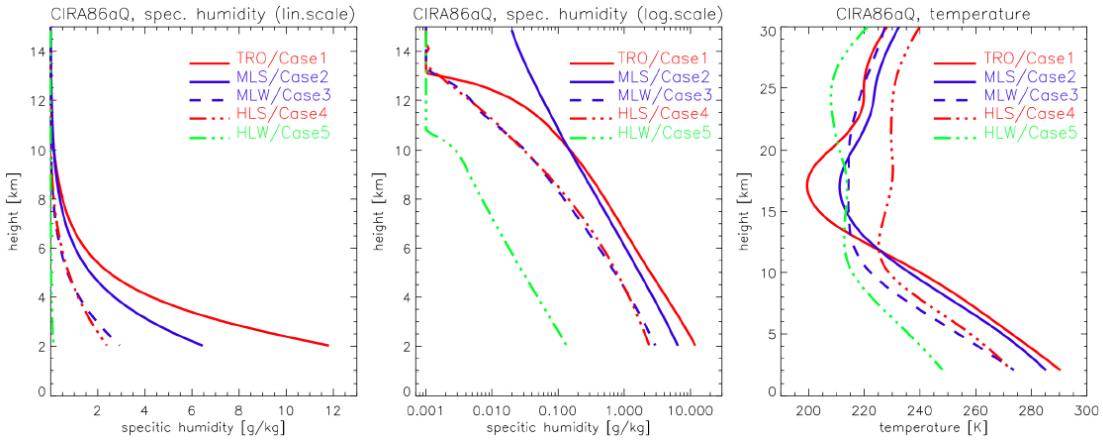

Figure 6.1: *Humidity and temperature profiles for five representative atmospheric cases of the CIRA86aQ model: tropical (TRO; July 0°N), mid-latitude summer (MLS; July 40°N), mid-latitude winter (MLW, January 40°N), high-latitude summer (HLS, July 70°N), and high-latitude winter (HLW; January 70°N) (Source: Kirchengast et al. 2004b).*

Five scenarios for different representative combinations of cloudiness and atmospheric turbulence have been defined to illustrate the performance under diverse conditions, which are summarised in Table 6.1. These cover conditions from clear-air, non-turbulent to cloudy and severely turbulent. For each scenario, an ensemble of 40 profile realizations was simulated in order to enable statistical performance estimates in terms of standard deviations and biases. The size of the ensembles was limited by the significant computational resources needed for the forward modelling of the simulated data, in particular for the high-accuracy ray-tracing and along-ray absorption integrations involved.

The retrieval performance for the clear-air, non-turbulent reference scenario is shown in Figure 6.2. The performance is found within target requirements at essentially all heights for both humidity and temperature. Figure 6.2 indicates the unique potential of the technique for determining unbiased humidity and temperature and its particular strength in the upper troposphere as already emphasized by Hoeg and Kirchengast (2002). Threshold height z_{Thres} (see Chapter 5, section LEO-LEO processing, on the meaning of z_{Thres}) was not reached in the atmospheric profile retrieval for this turbulence-free scenario, so no down-weighting of imaginary refractivities and best-fit temperature extrapolation from above z_{Thres} is involved.

1	**Clear-air, no turbulence**	(reference scenario)
2	**3D Cirrus clouds ('cCi1') plus 'high-latitude' turbulence ('sHL1')** C_{n0}^2 = 1 x 10^{-16} $m^{-2/3}$, H_{Cn2} = 2 km	*iwc* = 0.05 g/m^3 ± 0.025 g/m^3 (rms; 0–0.1 g/m^3) *c_height* = 8 km ± 0.5 km (rms; 7–9 km) *c_thickness* = 1.6 km ± 0.4 km (rms; 0.8–2.2 km)
3	**3D Altostratus clouds ('cAs1') plus 'mid-latitude' turbulence ('sML1')** C_{n0}^2 = 1.3 x 10^{-15} $m^{-2/3}$, H_{Cn2} = 2 km	*lwc* = 0.2 g/m^3 ± 0.1 g/m^3 (rms; 0–0.4 g/m^3) *c_height* = 4.5 km ± 0.25 km (rms; 4–5 km) *c_thickness* = 0.6 km ± 0.15 km (rms; 0.3–0.9 km)
4	**3D Cumulus clouds ('cCu1') plus 'subtropical' turbulence ('sST1')** C_{n0}^2 = 1 x 10^{-14} $m^{-2/3}$, H_{Cn2} = 1.5 km	*lwc* = 0.5 g/m^3 ± 0.25 g/m^3 (rms; 0–1 g/m^3) *c_height* = 2.5 km ± 0.25 km (rms; 2–3 km) *c_thickness* = 0.3 km ± 0.05 km (rms; 0.2–0.4 km)
5	**3D Cumulonimubus cloud and precipitation ('cCp1') plus 'tropical' turbulence ('sTR1')** C_{n0}^2 = 2 x 10^{-13} $m^{-2/3}$, H_{Cn2} = 1 km	*lwc* = 2.5 g/m^3 ± 0.5 g/m^3 (rms; 1.5–3.5 g/m^3) *c_height/lwc* = 2 km ± 0.25 km (rms; 1.5–2.5 km) *c_thickness/lwc* = 2 km ± 0.25 km (rms; 1.5–2.5 km) *iwc* = 0.15 g/m^3 ± 0.05 g/m^3 (rms; 0.05–0.25 g/m^3) *c_height/iwc* = 9 km ± 0.5 km (rms; 8–10 km) *c_thickness/iwc* = 3 km ± 0.5 km (rms; 2–4 km) *rr* = 20 mm/h ± 5 mm/h (rms; 10–30 km) *rr_topheight* = 2.5 km ± 0.25 km (rms; 2–3 km)

Legend: C_{n0}^2 … turbulence structure constant at surface, H_{Cn2} … scale height of turbulence structure constant, *lwc* … liquid water content (density) of cloud, *c_height* … centre height of cloud, *c_thickness* … thickness of cloud about centre height, *iwc* … ice water content (density) of cloud, *rr* … rain rate, *rr_topheight* … top height of rainfall. The horizontal extent of clouds was set to 200 km for *Ci* and *As*, 100 km for *Cu*, and 10 km for *Cp*. *Cp* has a gradual *lwc* decay over several kms above *c_thickness/lwc*. The horizontal extent of turbulence was set to 200 km in all cases and the vertical C_n^2 decay was assumed exponential with the scale height H_{Cn2}. The outer scale of turbulence was set to 100 m.

Table 6.1: *Parameters for cloud and turbulence scenarios.*

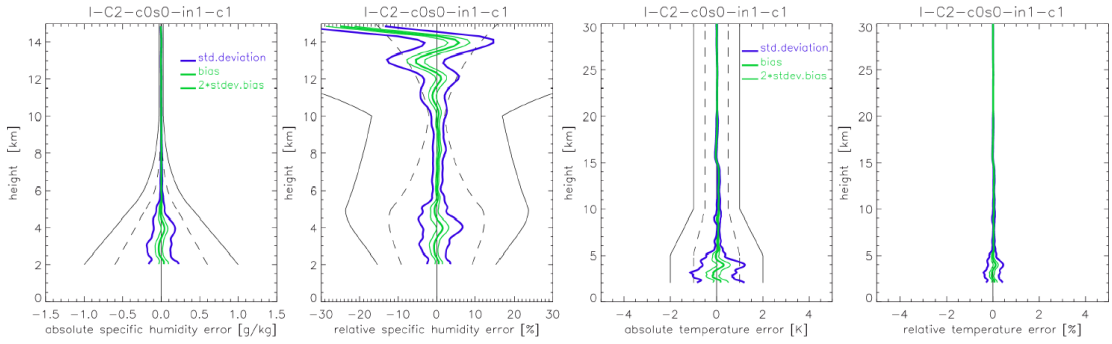

Figure 6.2: *Humidity (left panels) and temperature (right panels) retrieval error results for the clear-air, non-turbulent scenario. Statistical performance results are shown (standard deviation, bias, 2 x std. deviation of bias), with the std. deviations depicted as +/– envelopes around the bias profiles. In the left and two middle panels, the observational requirements, as laid out in chapter 4, are shown for reference (solid black, threshold requirements; dashed black, target requirements). The small temperature residual bias of up to 0.1 K visible below 15 km in this and the following Figures 6.4 and 6.7– 6.9 is a small technical weakness only of the present, not yet fully optimized end-to-end simulation, as is a significant fraction of the 'error oscillation' above about 12 km in the relative humidity error (Source: Kirchengast et al. 2004b).*

The possible impact of scintillation resulting from tropospheric turbulence must be considered in the performance evaluation. In order to estimate the possible magnitude of turbulences, multi-year, high-resolution radiosonde data sets from different latitudes, from tropical to high latitudes, have been analysed to obtain good estimates of profiles of the refractive index structure constant (C_n^2) and its statistics as a function of latitude (Sterenborg and Poiares-Baptista, ESA/ESTEC, pers. comm. 2003). The C_n^2 profiles are needed for the calculation of scintillation effects. Sample results are shown in Figure 6.3 and were found consistent with respective literature evidence on C_n^2 from turbulent scatter radars, in-situ refractometers (e.g. Gage 1990, Gossard 1990), and low-resolution radiosonde data (e.g. Vasseur 1999). They have been used as a guideline to define reasonable average (median) turbulence cases for the present performance analysis.

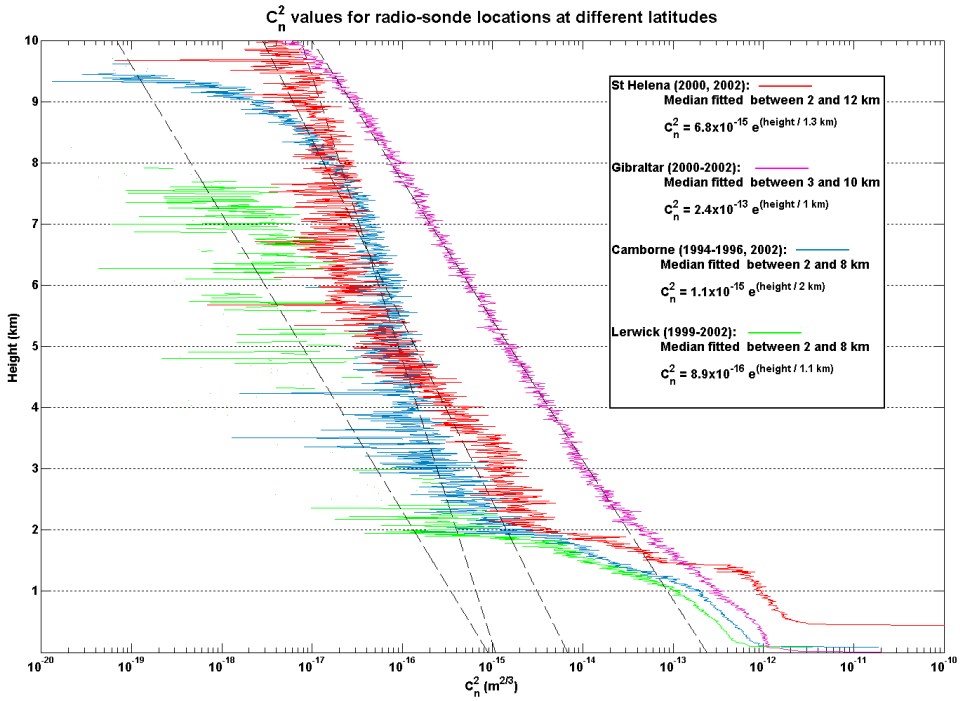

Figure 6.3: *Sample empirical median C_n^2 profiles, and associated best log-linear fits, derived from multi-year high-resolution radiosonde databases at different latitudes.*

The cloud parameters used largely followed Gradinarsky et al. (2003), who compiled from literature typical properties of the different cloud types, and were essentially modelled as simple horizontally-limited layers with constant liquid water or ice water content within the given thickness about the given cloud height. The clouds were assumed centred at the occultation event (mean tangent point) location, ensuring that the occultation signals passed through them. Randomized selection of the cloud parameters within the given bounds was performed to obtain different clouds for the individual realizations in an ensemble, mimicking cloud variability. Every second event in each ensemble was assumed cloudy, mimicking an average cloud coverage of 50%.

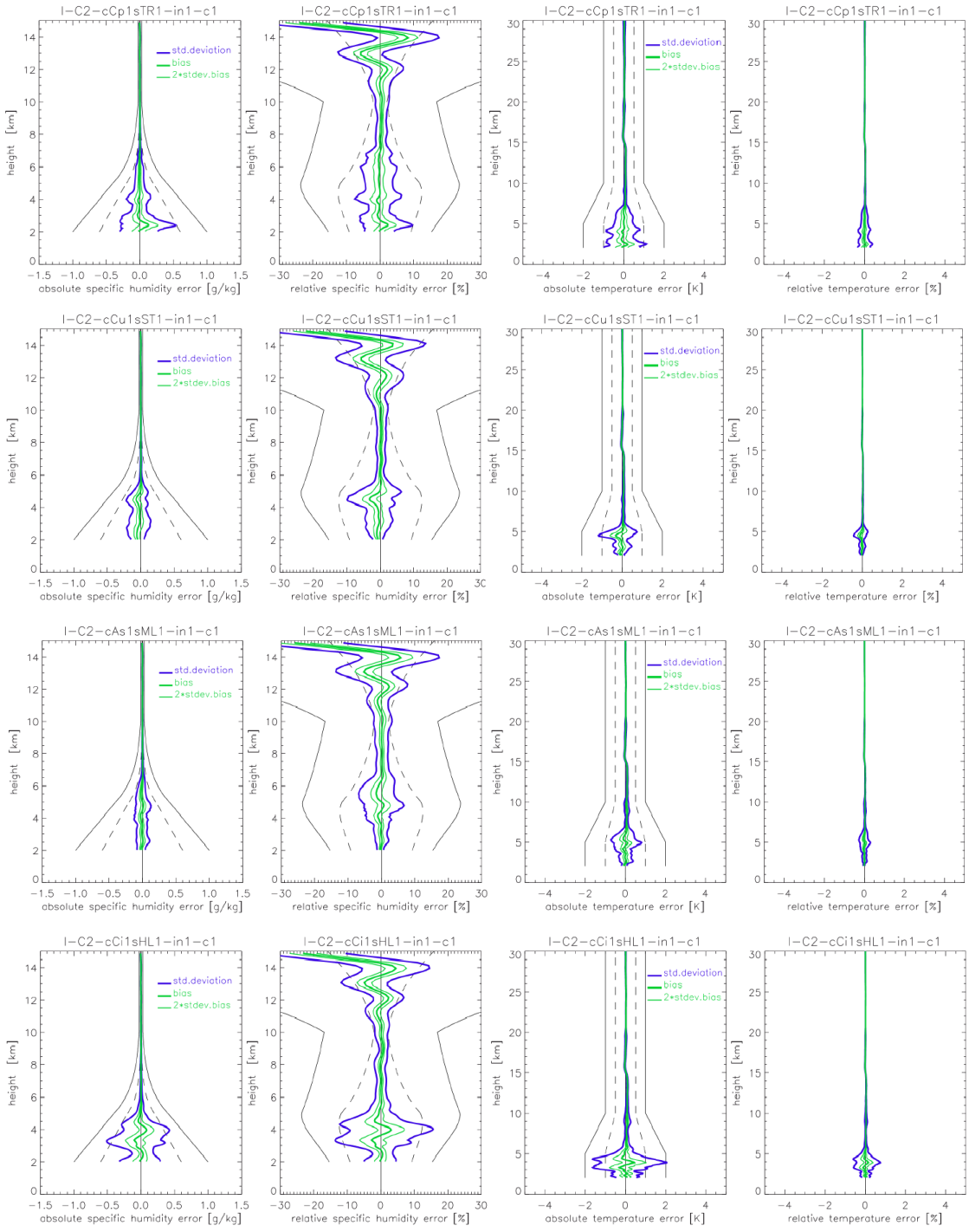

Figure 6.4: *Humidity (left panels) and temperature (right panels) retrieval error results for the four cloudy, turbulent air scenarios of Table 6.1. Each row depicts one scenario (top, 'tropical'; 2nd, 'subtropical'; 3rd, 'mid latitude'; bottom, 'high latitude'). Figure layout same as Figure 6.2 (see that caption for details). (Source: Kirchengast et al. 2004b).*

Figures 6.4 show humidity and temperature performance results for the four representative cloudy and turbulent scenarios of Table 6.1. All scenarios are found to be within target requirements and unbiased at almost all heights (Kirchengast et al. 2004b). The upper troposphere between about 6 and 12 km is found to be particularly accurate, with specific humidity errors generally smaller than 5%. In the lower troposphere, the high-latitude scenario, influenced by the weakest turbulence, exhibits the comparatively largest errors. This is due to the fact that turbulence is now present, but that for the given turbulence strength still no threshold height z_{Thres} is reached in most of the realizations of the ensemble, so that almost no auxiliary temperature information is utilized. The different liquid water clouds are found not to pose significant problems for the retrieval. The presumed insensitivity to ice clouds is found to be confirmed (see also Gradinarsky et al. 2003), which is important for several science objectives noted in Chapter 3. Significant rain is found to strongly impact the absorption and to lead to z_{Thres} being above the top of rain, so that the latter has an effect analogous to severe turbulence. Significant rain rates above 2-3 km height are rare, however.

6.1.2 ECMWF Operational Analysis Cases

As a quasi-realistic performance analysis case, an operational T511L60 analysis (~40 km × 40 km horizontal resolution, 60 vertical levels from surface to 0.1 hPa) of the ECMWF was used (12 UTC analysis of Sept. 15, 2002; near-equinox date, otherwise arbitrarily chosen). A global set of about 115 occultation events was simulated (the number limited by the computationally expensive forward modelling, as in the previous section), drawing every second event from a day of LEO-LEO measurements, and sorting the events into three latitude bands (low, mid, high). Figure 6.5 illustrates the coverage by ACE+ LEO-LEO occultation events for a baseline 4-satellite constellation (~230 profiles/day) and shows the global distribution of the selected events falling into both cloudy and clear-air areas.

Besides humidity and temperature, ECMWF analyses also contain 3D liquid water and ice water cloud fields, which were included in the modelling. Figure 6.6 illustrates, via a latitude-height cross-section at 0 deg longitude (Greenwich meridian), the variability of the humidity, temperature, liquid water, and ice water fields in the analysis used. The vertical humidity and temperature profiles at each event location have been used, disregarding the horizontal variation about this location. This was done to clearly quantify the observational and retrieval errors and to avoid mixing in representativeness errors. The latter are small given properly defined ‘true’ profiles (e.g. Foelsche and Kirchengast 2004, Syndergaard et al. 2004). The present LEO-LEO end-to-end simulator could not yet supply adequate Abelian-weighted ‘true’ profiles, but only vertical profiles. The 3D liquid water and ice water fields have been used as they are, and contribute to the absorptive occultation signal at any location where occultation rays pass through cloudiness.

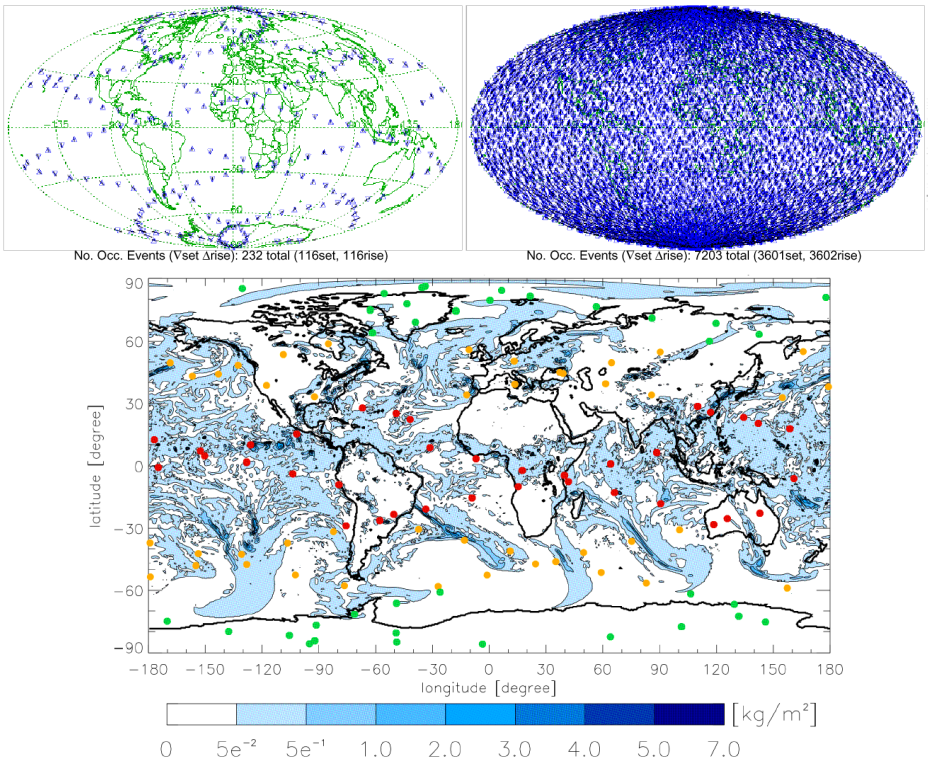

Figure 6.5: *Coverage by LEO-LEO occultation events for the baseline 4-satellite constellation. Top-left: daily coverage; Top-right: monthly coverage; Bottom: coverage used in the simulations, including every second daily event sorted into low (red dots), middle (orange dots), and high (green dots) latitude bands of 30 deg width each. The background shows the vertically integrated liquid water density (units g/m²) indicating cloud coverage (data from Sept. 15, 2002, 12 UTC, ECMWF analysis). (Source: Kirchengast et al. 2004b)*

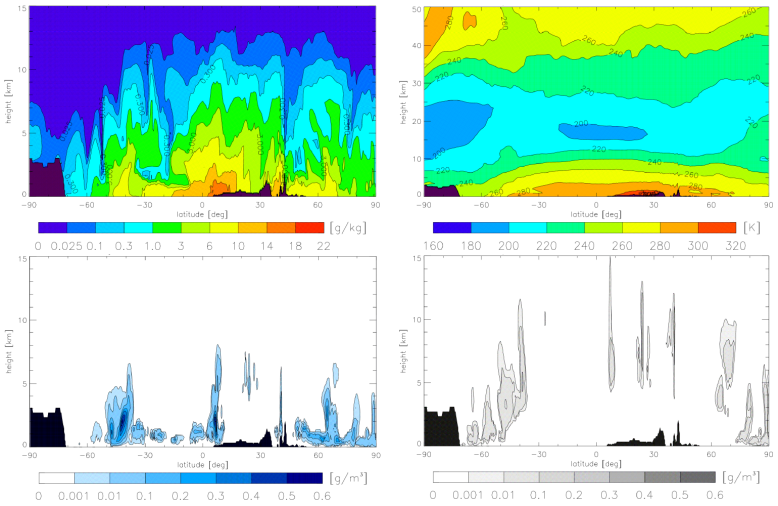

Figure 6.6: *Specific humidity (top-left), temperature (top-right), liquid water density (bottom-left), and ice water density (bottom-right) latitude-height cross sections at 0 deg longitude through the ECMWF analysis used in the simulations (analysis of Sept. 15, 2002, 12 UTC). (Source: Kirchengast et al. 2004b)*

Regarding turbulence/scintillations, the same model as with the CIRA86aQ cases was used (Sterenborg and Poiares-Baptista, ESA/ESTEC, pers. comm. 2003), but with the main turbulence parameters modelled as a function of latitude based on the turbulence cases as defined in Table 6.1. The values of C_{n0}^2 and H_{Cn2} were assigned to latitudes (both North and South) of 0 deg ('TR1'), 20 deg ('ST1'), 50 deg ('ML1'), and 70 deg ('HL1'), complemented by values of ($C_{n0}^2 = 3 \times 10^{-15}$ m$^{-2/3}$, $H_{Cn2} = 1.75$ km) at 30 deg to better reflect subtropical dry and weakly turbulent areas (ACE+ MAG, pers. comm. 2004). In between, linear interpolation was performed, and beyond 70 deg values were kept constant at the 70 deg values. If due to turbulence best-fit background temperatures needed to be invoked below z_{Thres} (see Chapter 5 for details), temperature profiles from the ECMWF 24h forecast for the analysis time were used as a 'search library', searching within a few degrees around the given event location. A conservative uncertainty of 0.75 K (near z_{Thres}) to 2 K (near 2 km) was then attached to the best-fit background profile.

Figures 6.7 to 6.9 show the performance results for the three latitude bands, each containing an ensemble of about 30-40 occultation events (cf. Fig. 6.5). Not all profiles reach fully down to 2 km, partly due to topography, partly due to multipath effects in the lower troposphere limiting the ray-tracing. Future more elaborated (and computationally expensive) wave-optics forward modelling is expected to cope with the latter effects. From GNSS-LEO experience, however, the performance indicated here using ray-tracing forward modelling will not change much (tentatively it will be improved).

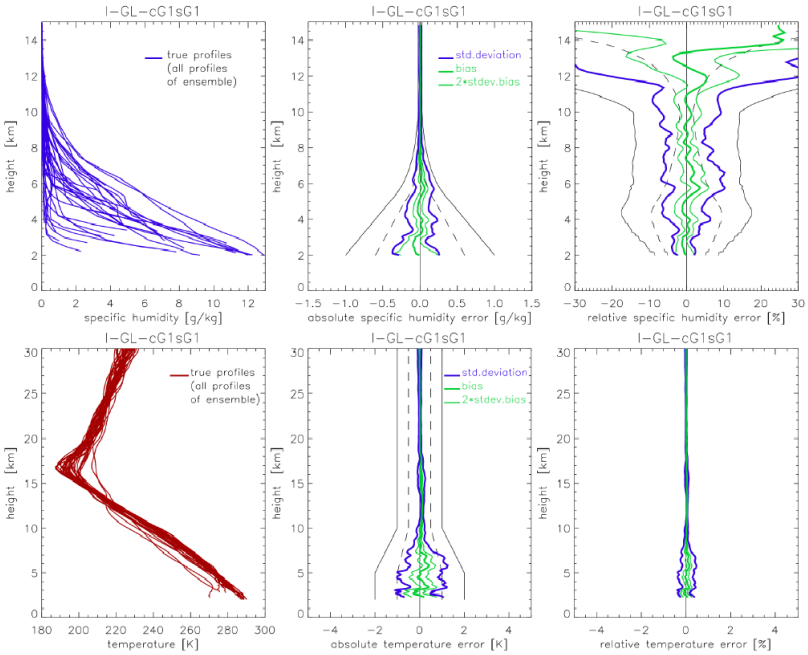

Figure 6.7: *Humidity (top) and temperature (bottom) 'true' profiles (left panels) and retrieval error results (middle and right panels) for the ECMWF low-latitude ensemble. Error result panels layout as for Figure 6.2, see that caption for details. (Source: Kirchengast et al. 2004b)*

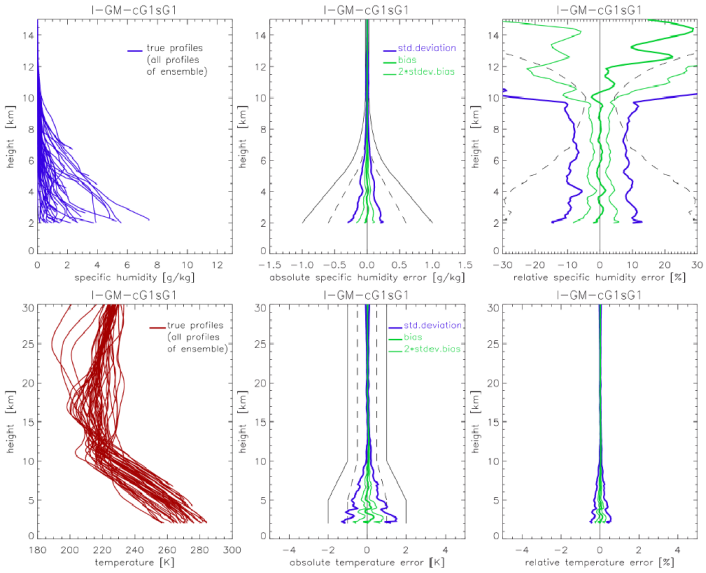

Figure 6.8: *Humidity (top) and temperature (bottom) 'true' profiles (left panels) and retrieval error results (middle and right panels) for the ECMWF mid-latitude ensemble. Same layout as Figure 6.7. (Source: Kirchengast et al. 2004b)*

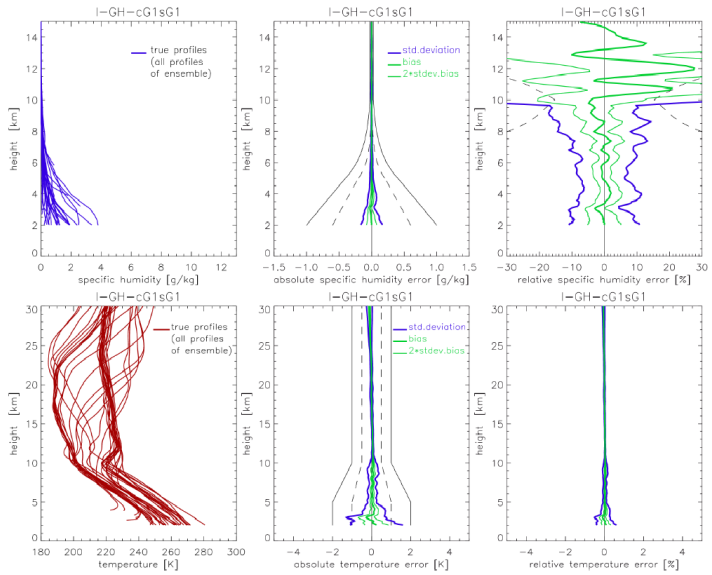

Figure 6.9: *Humidity (top) and temperature (bottom) 'true' profiles (left panels) and retrieval error results (middle and right panels) for the ECMWF high-latitude ensemble. Same layout as Figure 6.7. (Source: Kirchengast et al. 2004b)*

The left panels of Figures 6.7 to 6.9 illustrate the wide variety of atmospheric humidity and temperature conditions covered by the profiles. The humidity error panels show that the performance is in general found to be within target requirements below about 6 to 10 km; above, it is close to target and well below threshold requirements. No significant biases are found at any height and the humidity RMS error up to near 10 to 12 km, dependent on latitude, is found within about 10%. Above 10 to 12 km, a

considerable fraction of the errors can be attributed to the not yet fully optimized LEO-LEO end-to-end simulator, in particular to improvement potential in the filtering and weighting of transmission and imaginary refractivity data and to the humidity cut-off (to zero) at 15 km by the current atmospheric models inherited from the GNSS-LEO end-to-end simulator (holds for both the CIRA86aQ model and for the current 'GCM 3D Atmosphere' model accessing and interpolating the ECMWF analyses). The temperature performance is found to be unbiased and within target requirements essentially at all heights for all three latitude bands.

Figure 6.10 illustrates, using retrieval error-to-background error ratios as an instructive diagnostic (e.g. Rodgers 2000, Rieder and Kirchengast 2001), the independence of the baseline retrieval ($z_{\mathrm{Thres}} = 0$; see Chapter 5 for details) from background information as well as how background temperature information comes in below about 3 to 6 km dependent on the severity of atmospheric turbulence. Error ratios well below 0.1 imply that essentially all information comes from the measurements, whilst ratios > 0.5 indicate that the majority of information comes from the background. The error ratio profiles of the clear-air, no-turbulence reference scenario (shown in Figure 6.2) demonstrate that background plays no role in the baseline retrieval. The error ratios of the ECMWF ensembles for the three latitude bands, with strongest turbulence modelled at low latitudes and weakest at high latitudes, indicate how the different z_{Thres} of individual events lead on average to temperature background information becoming important (ratios > 0.5) below about 3 km (high latitudes) to 6 km (low latitudes). This is consistent with expectations related to the severity of turbulence (cf. Chapters 4 and 5), whereby it is to be re-called that here the most conservative case of fully height filling turbulence below z_{Thres} was modelled. Water vapour error ratios are always about zero, independent of whether temperature background is used or not, since water vapour background is never used. At the heights where temperature background is used, the humidity retrieval is mainly based on the real refractivity measurements plus the background temperature. The loss of usability of the imaginary refractivity signal (due to scintillation) below z_{Thres} leads, however, to significant correlations in the retrieved temperature and water vapour errors. Figures 6.7 to 6.9 show that the humidity and temperature retrievals are unbiased also at these heights, which is ensured by the best-fit to the retrieved temperature data above z_{Thres} and the quality of the 'search library' (24h forecasts).

In summary, the LEO-LEO performance is found to be compliant with the requirements laid out in Chapter 4. Compared to GNSS-LEO with its tropospheric temperature-humidity ambiguity, the simultaneous availability of accurate humidity, temperature, and pressure as a function of geometric height from LEO-LEO is a particularly intriguing property. Also, the best-fit temperature extrapolation from above z_{Thres} in case of severe turbulence in the lower troposphere is a simple method that is found to be adequate for retrieval under these adverse conditions.

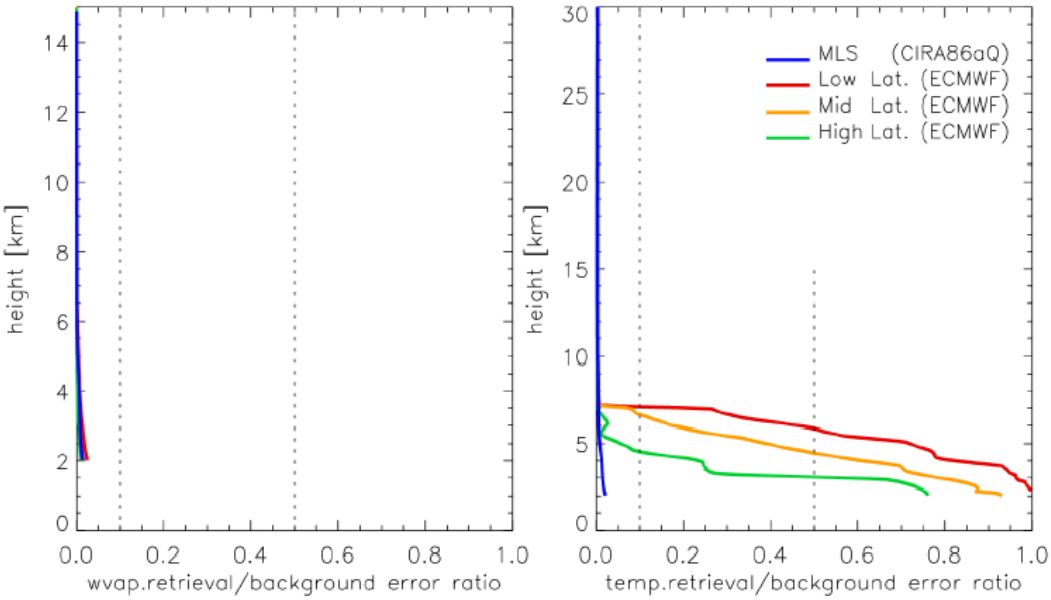

Figure 6.10: *Retrieval error-to-background error ratios for retrieved water vapour (left panel) and temperature (right panel) profiles for the clear-air, non-turbulent reference scenario of Figure 6.2 (blue), and the ECMWF low-latitude (red), mid-latitude (orange), and high-latitude (green) ensembles. Baseline background uncertainties in the BLUE algorithm have been set to 100 K and 25 mbar for temperature and water vapour, respectively, for the results presented, but could have been set to any other 'quasi-infinite' values, which ensure the BLUE being entirely driven by the measured refractivities only. (Source: Kirchengast et al. 2004b)*

6.2 GNSS-LEO Occultation Performance

The performance of GNSS-LEO occultations is well established due to the strong heritage of the observation principle and dedicated studies for the previous ESA GNSS occultation mission candidate and other previous missions. Starting with the successful GPS/MET 'proof-of-concept' within 1995–1997 (e.g. Rocken et al. 1997), the GNSS-LEO technique was extensively evaluated and detailed descriptions of the method and its scientific performance are available from literature (e.g. Kursinski et al. 1997, Lee et al. 2001, Steiner et al. 2001, Hajj et al. 2002, Steiner and Kirchengast 2004, and references therein). These sources confirm the compliance of GNSS-LEO retrievals with the requirements of Chapter 4. Thus for brevity only one illustrative climate-related performance result is included here. For climate change analyses based on GNSS-LEO data, refractivity, dry temperature, and geopotential height are particularly promising variables. As an example, Figure 6.11 illustrates the dry temperature accuracy (left panel) and indicates that climate trends expected over the coming decades (right panel) will be reliably measurable by GNSS-LEO data thanks to their accuracy and long-term stability.

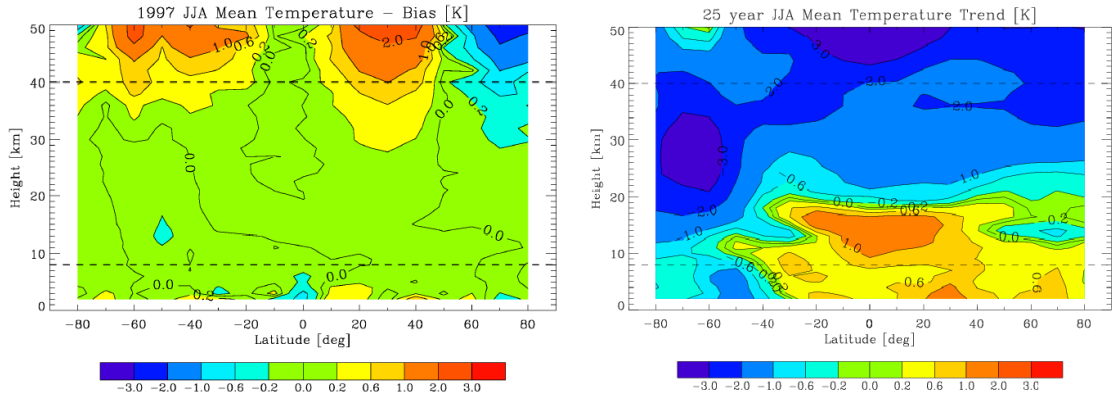

Figure 6.11: *Latitude-height slice of climatological residual bias errors in average profiles of dry temperature in 17 latitude bins of 10° width from 80°S to 80°N (left panel) compared to 25-yr summer temperature trends from 2001–2025 in the same bins (right panel). Each average profile in the left panel involves ~50 realistically simulated individual GNSS-LEO occultation profiles sampled by an ACE+-type satellite constellation within a full summer season (June-July-August). The trends in the right panel are derived from a recent climate model simulation with the Hamburg ECHAM5 model at T42L39 resolution (top at 0.01 hPa). (Source: Univ. of Graz)*

Within the ACE+ concept, the GNSS-LEO data are an important complement to the LEO-LEO data in that they vastly enhance the number of occultation profiles per day and thus contribute importantly to the scientific objectives, as is made evident also in the following section.

6.3 Climate Variability and Trends Measurement Performance

The performance in measuring climate variability and trends over the mission lifetime has been assessed in form of a check on how adequate the ACE+ coverage is, together with the accuracy demonstrated in the subsections above, in order to reach a required climatological accuracy. As basis for the check, two 5 year climate simulations were run with the Hamburg ECHAM5.2/MA model (Kornblüh, pers. comm. 2004, Roeckner et al. 1999, Kirchengast et al. 2004b).

Based on the 5 years of model run output fields, humidity and temperature profiles were sampled at all ACE+ LEO-LEO and GNSS-LEO occultation event locations occurring over a 5-year mission lifetime. The along-ray horizontal resolution of about 300 km was accounted for in this sampling, in that not just local but ‘along-ray weighted’ profiles were extracted at each event location. The ACE+ mission used was the full 4-satellite constellation (cf. Chapter 4), and reduced configurations with 3 and 2 satellites for comparison. The extensive sets of event locations were computed from 5-years ACE+ geometry simulations with the EGOPS end-to-end simulator propagating the satellites with a long-term accurate Keplerian orbit propagator. Before constructing climatologies, the sampled humidity and temperature profiles were

superposed with random errors statistically consistent with the expected LEO-LEO and GNSS-LEO accuracy. ACE+-observed climatologies were then constructed based on the sampled profiles and compared with the 'true' climatologies computed from the climate model output at full resolution.

Here global-mean performance results are shown at the 300 hPa level (~9 km) and the 500 hPa level (~5 km), respectively. The climatological accuracy required to reasonably capture climate variability and trends at these levels has been defined, from experience, as 0.1 K for temperature and 5% for specific humidity at 300 hPa, and as 0.2 K and 5% at 500 hPa.

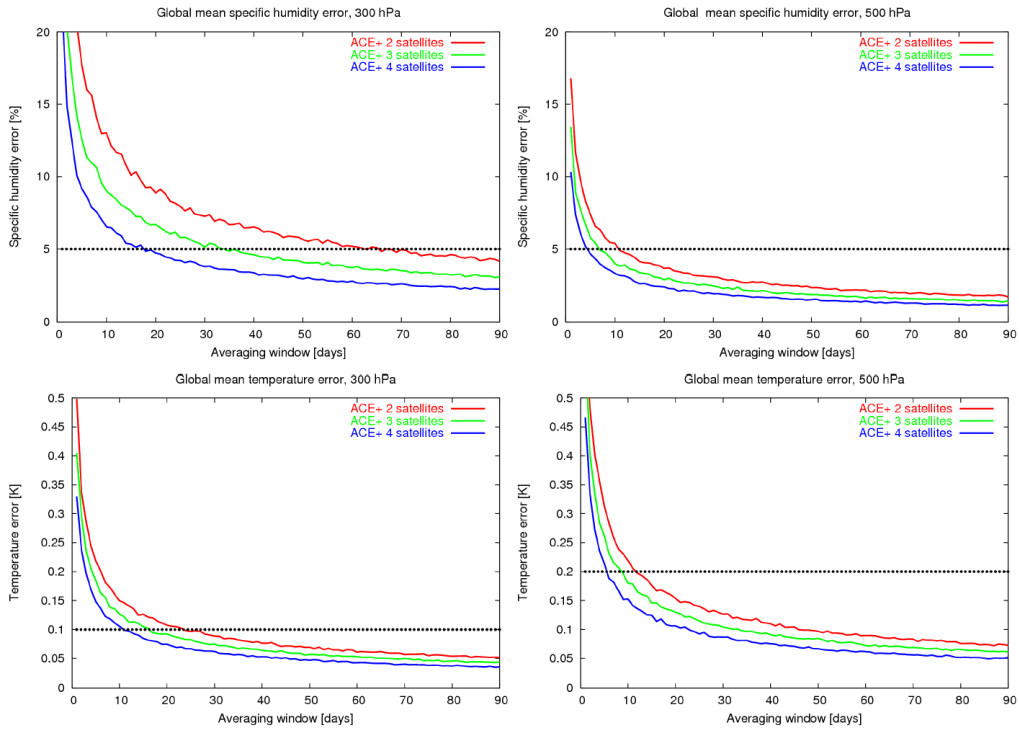

Figure 6.12: *Global-mean climatological specific humidity (top) and temperature (bottom) errors at 300 hPa (left) and 500 hPa (right) as a function of averaging interval. Results for four (blue), three (green), and two (red) ACE+ satellites are shown and a climatological accuracy desired within < 30 days is indicated (dotted horizontal). (Source: MPI for Meteorology)*

Figure 6.12 shows, for the 3 different ACE+ constellations assumed, the global-mean humidity and temperature errors in the ACE+-observed climatologies relative to the 'true' climatologies as a function of the averaging time window up to a seasonal average (90 days). The error level for a time window of one month is a good indicator for sufficient spatial coverage with respect to measuring variability and trends. The smaller the errors within 30 days are, the better for climate applications. It is desirable that the defined climatological accuracies are reached within 30 days. For humidity, the

achieved accuracy at the 300 hPa level is dominated by the LEO-LEO data (since GNSS-LEO sensitivity to humidity above 8 km is generally negligible), whilst at 500 hPa the GNSS-LEO data dominate due to their large number (> 4000 GPS/GALILEO occultations per day, ~230 LEO-LEO occultations per day). The upper tropospheric humidity is of particular interest, however. It is found that a 4-satellite constellation is mandatory to achieve the 5% climatological humidity accuracy within one month; the 2-satellite constellation requires more than two months of sampling to achieve it. For temperature, to which both GNSS-LEO and LEO-LEO contribute important information, the required accuracies are achieved well within one month. This indicates significant climate information potential also at regional scales.

Overall, the estimated climate measurement performance of the ACE+ baseline constellation, thanks to both its LEO-LEO and GNSS-LEO components, is expected to meet the climate scientific objectives laid out in Chapter 3.

7. User Community Readiness

The user community of ACE+ observations covers a variety of research fields such as climate science, meteorology, and aeronomy. Most of the research groups in these areas are aware of the benefits of GNSS-LEO data for determining the basic parameters such as profiles of temperature, pressure, humidity, refractivity, and bending angle. Since the new and novel LEO-LEO measurements deliver similar Level 2 data products, with the emphasis on accurate humidity profiles, the research user community will immediately be capable of exploiting these ACE+ observations.

The ACE+ mission is based on comprehensive scientific and technical ESA studies since 1995 (Høeg et al. 1995), especially from recent ESA studies and previous proposed satellite projects as the Earth Explorer Opportunity Mission ACE (Høeg and Leppelmeier 2000) and the Earth Explorer Core Mission WATS (ESA 2001). A European scientific core team of more than 10 institutions and a worldwide Science User Team of more than 20 institutions supported the ACE+ proposal (Høeg and Kirchengast 2002, Kirchengast and Høeg 2004). The institutions and universities interested in ACE+ (covering European researchers and entities, together with international research groups and organisations) are listed in the appendix to the ACE+ proposal (Hoeg and Kirchengast 2002). Scientific projects that they wanted to initiate once the ACE+ data become available are defined clearly.

The user groups fall into four general categories:

- *Science individual users and institutions*, with a high level of knowledge of the capability of the measurements and their assumptions/limitations for the GNSS-LEO measurements as well as the LEO-LEO observations. This is the main target user community according to the mission objectives.
- *NWP users*, exploiting the observations within meteorology and weather forecasting – mostly through data assimilation of products such as refractivity (real and imaginary), humidity, temperature, pressure, bending angle, and transmission profiles.
- *Public and educational users*, benefitting from the database of troposphere and stratosphere observations for student science projects and for general information material describing the state and development of the Earth's atmosphere.
- *Added-value community*, who will use the information in the higher level data products (2 and 3), where global standard parameters are made available either as the sole information, as calibration for, or as complement to other measurements (humidity, temperature, pressure, clouds, turbulence, electron densities, radiation, geostrophic winds, thermodynamic conditions, etc.).

The major users of the observations fall into the first category. They will be able to extract the full information content of the state-of-the-art LEO-LEO measurements, which will be the first of their kind.

8. Global Context

The ACE+ mission will contribute to a number of international programmes, in particular those focusing on climate research. It will be highly complementary in time, coverage and observed geophysical quantities to other presently ongoing or planned missions on climate change, particularly those focusing on atmospheric dynamics, radiation and chemistry, and the global water cycle.

ACE+ will be highly supportive to the World Climate Research Programme (WCRP) whose main objectives are to observe, understand, model, and predict climate variations and long-term changes. In particular the WCRP research projects CLIVAR, GEWEX and SPARC will benefit from the ACE+ measurements. CLIVAR aims at improving our understanding of those physical processes in the climate system that are responsible for climate variability on time scales ranging from seasons to centuries. CLIVAR considers natural variability as well as anthropogenic influences on climate change. GEWEX focuses on observation, understanding and modelling of the hydrological cycle and energy fluxes in the atmosphere. The goal of GEWEX is to reproduce and predict variations in the global hydrological regime, its impact on atmospheric and surface dynamics, and variations in regional hydrological processes and water resources and their response to changes in the environment, such as the increase in greenhouse gases. SPARC analyses stratospheric processes and their impact on the climate system. The assessment of water vapour in the stratosphere and the upper troposphere is an important SPARC initiative.

ACE+ also responds to the needs of the Global Climate Observing System (GCOS, co-sponsored by WMO, IOC, UNEP and ICSU), namely its climate system monitoring and trend detection objectives. The measurements of the LEO-LEO component will be very valuable in providing absolute humidity, and will also provide a benchmark for the calibration and inter-calibration of other satellite missions contributing to GCOS. Furthermore, ACE+ would contribute to the Global Observing System (GOS) of the WMO core activity World Weather Watch (WWW).

COST Action 723

The importance of improving the quality of upper tropospheric humidity data has also been recognised by the European Commission. ‘COST Action 723: Data Exploitation and Modelling for the Upper Troposphere and Lower Stratosphere’ had its Opening Workshop in March 2004 at ESA/ESTEC, Noordwijk. ‘Working Group 1’, dealing with data, has a strong focus on water vapour. It includes specialists for the different established measurement techniques, such as in-situ measurements by capacitive sensors (Vaisala RS80), as well as the various surface, aircraft, and satellite based remote sensing techniques. One of the aims of the Working Group is to improve the quality and absolute accuracy of humidity data by systematic inter-comparison studies and campaigns. Consolidation of the different humidity sensors is perceived as an urgent issue.

COST Action 716, EUMETNET, and Ground-Based GNSS

Another European activity relevant to the ACE+ mission is 'COST Action 716: Exploitation of Ground-Based GPS for Climate and Numerical Weather Prediction Applications' (http://www.oso.chalmers.se/geo/cost716.html) and its follow-on activities. The COST action itself ends during 2004 and a proposal to EUMETNET is now being written in order to make a continued use of the ground-based GPS networks producing integrated amounts of the water vapour above each GPS site. These data have two main applications, namely in forecasting and climate research. Water vapour results available in near real time will be complementary to the ACE+ near real time humidity profile information, which have excellent accuracy in the upper troposphere, but will have difficulties in reaching the ground surface where water vapour is most abundant. For climate research, ACE+ will provide details about the vertical profile of water vapour, and the ground-based GPS data will add the important constraint on the integrated amount. The global network processed by the International GPS Service (IGS, http://igscb.jpl.nasa.gov) now consists of more than 300 sites, and much denser regional networks exist in Europe, North America, and Japan.

Other Radio Occultation Missions

GNSS-LEO radio occultations have now been carried out for almost a decade. GPS/MET was the first proof-of-concept mission to deduce and validate stratosphere and troposphere temperature and pressure profiles in 1995. Since then several missions have enhanced the findings of GPS/MET. The future will see two operational missions, consisting of satellites following each other in time (EPS/MetOp and NPOESS; the latter might embark a GPS occultation instrument), and several scientific missions (see Fig. 8.1). Evidently, ACE+ is a leading element during its scheduled timeframe.

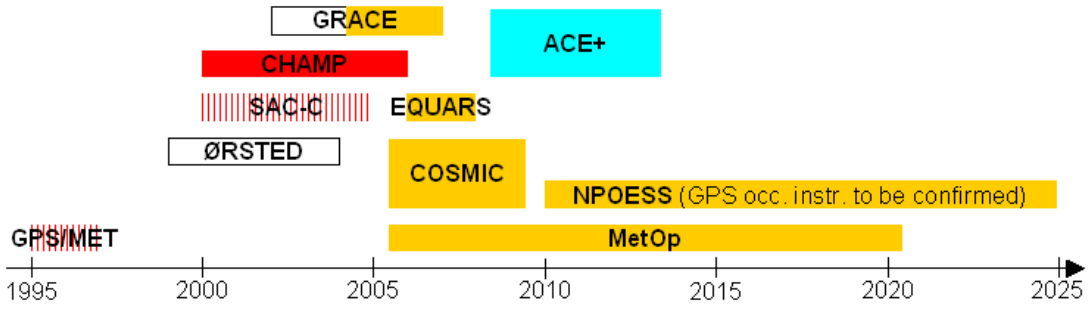

Figure 8.1: *Past and future GNSS-LEO radio occultation missions. Colour code: red=useful GPS-LEO data acquired (red-striped, campaign-wise only), white=no useful data acquired, yellow=approved missions, and blue=the proposed ACE+ mission with first GALILEO-LEO data and novel LEO-LEO phase and amplitude occultation data.*

The X/K-band (LEO-LEO) occultation of ACE+ is new, both for phase and amplitude, and has not been accomplished and is not being planned on any other satellite mission.

Other Satellite-based Humidity Sensors

Remote sensing systems for retrieving humidity information can be characterised based on the frequencies and the geometries used.

Infrared down-looking instruments (e.g. HIRS and AIRS/IASI)

The vertical resolution is several kilometres for the older instruments and 1–2 km for the Infrared Atmospheric Sounding Interferometer (IASI). The influence of radiation from clouds is the main difficulty when using infrared instruments. Retrievals can only be made down to the top of the cloud, provided that the vertical resolution is high enough to suppress the cloud influence. There are large amounts of measurements available. The TOVS archive dates back to 1978 (Soden et al. 2004), although uncertainties about the absolute calibration limits their usefulness for long-term trend studies.

Microwave downward-looking instruments (e.g. SSM/I, AMSU)

The majority of the existing humidity data are obtained on and around the 22 GHz and 183 GHz water vapour lines. Using several frequencies, it is possible to make corrections for the emission from clouds. On the other hand, these instruments have very coarse vertical resolutions and there are problems with the background radiation. Therefore, they mainly provide useful integrated amounts of water vapour data over the oceans, where algorithms for the ocean surface brightness can be developed. Microwave radiometers operating around the 183 GHz line have difficulty in sensing through liquid clouds.

Microwave limb-sounding instruments (e.g. EOS/MLS)

Microwave limb sounding provides a good vertical resolution, determined by the size of the antenna and the frequency. These instruments produce a lot of data with global coverage, but absolute calibration with high accuracy is difficult. The emission data acquired at 180 GHz have their strength in the lower stratosphere, and will saturate in the middle troposphere and below.

Solar occultation instruments (e.g. HALOE)

Water vapour data have been produced since 1991 covering the height interval from 12 to 35 km with a vertical resolution of approximately 2 km and an uncertainty of 10–15% (Park et al. 2004). However, as for all optical and infrared instrumentation, no

retrieval is possible if clouds are present in the signal path. Solar occultations provide only very limited geographical coverage and are limited to sunrise/sunset.

The ACE+ orbits will be in the same orbital plane as the MetOp orbit. This will allow the provision of highly complementary and synergistic measurements of water vapour, particularly in the upper troposphere, with IASI, HIRS-4 and AMSU.

9. Application Potential

ACE+ has been designed with the stated climate research objectives as its main drivers. In addition, however, ACE+ data can be used and will be highly welcome in other research and application areas, as outlined below.

9.1 Weather Forecasting and Atmospheric Analysis

Most obviously, ACE+ will be highly valuable for weather forecasting, if the data products are delivered in nearly real time. At present, observational information on the three-dimensional humidity and temperature over the oceans and in the tropics is limited to a few radiosonde stations, and the relatively inaccurate and coarse vertical soundings of humidity and temperature from the orbiting NOAA satellites. This severely limits predictability over the European continent for synoptic disturbances developing over the North Atlantic Ocean.

There are numerous examples of forecasts missing severe extra-tropical low-pressure systems, which can be ascribed to the lack of or incomplete upper air information over the ocean to the west of Europe. Therefore, deficiencies in the current observing system degrade present day weather forecasting. Not only improved humidity and temperature observations are needed to improve the weather prediction skills; information on the mass and wind fields has to be available when modelling the atmospheric state.

The atmospheric mass field, characterised by temperature, pressure, and water vapour, dominates the main features of the large-scale atmospheric wind systems via the geostrophic balance. This, together with the fact that massive amounts of latent heat are transported, via the dynamics of the atmosphere, and released in areas of condensation, underlines the importance of water vapour and temperature in controlling the atmospheric circulation.

In the tropics, information about the wind field is, in general, relatively more important than mass field information. However, for synoptic and larger scale disturbances in the extra-tropical regions, there is little doubt that high quality mass field observations over the oceans are the main factor limiting the skill of operational numerical weather prediction systems. the fact that data delivery from ACE+ is planned to occur within a 3-hour time window for a significant fraction of the data makes the mission very attractive for weather forecasting and atmospheric analysis.

9.2 Tropospheric Turbulence

Atmospheric turbulence influences how energy is transformed from large-scale features in the input range through the turbulence range, where eddies are broken up into smaller and smaller sizes, into the dissipation range, where the energy is converted into heat. The turbulence range spans scales from the order of 100 metres down to a

few centimetres. Our knowledge about the amount of turbulence in the troposphere and lower stratosphere is mainly obtained from radar observations at a few sites (e.g. Rao et al. 2001). Turbulence models, using the vertical profile of the refractive index as input data, agree in a statistical sense with observations, and have been validated at particular sites where radiosondes are launched and radars or satellite beacon receivers are located (e.g. Vasseur 1999). The information on the global distribution of turbulence is therefore rather poor. ACE+ will provide a completely new and independent data set for assessing the tropospheric turbulence, with global coverage and a unique geometry defined by the microwave link between the LEO satellites.

9.3 Ionosphere and Space Weather

The Earth's ionosphere, ranging from about 90 km up to the bottom of the plasmasphere at about 1000 km, is strongly subjected to space weather phenomena characterised by highly variable solar driven forces such as solar radiation, solar wind, electric fields and currents, thermospheric winds, and particle precipitation. Since the ACE+ mission includes the ability to yield unique information about the ionosphere on a global scale via GNSS-LEO occultations, it will significantly contribute, as a spin-off, also to space weather services planned in the frame of the European Space Weather Programme (ESWP) during the next decade. Furthermore, the ionospheric data can be used to improve ionospheric correction algorithms applied in neutral gas retrieval procedures to derive excellent upper stratosphere data.

Reliable nowcasting and forecasting of space weather phenomena require improved understanding of the ionosphere's behaviour and its close coupling with the magnetosphere and thermosphere systems. Applying innovative inversion techniques, data assimilation methods, and tomographic approaches will allow us to monitor and model space/time electron density structures on global and regional scales with high reliability and accuracy as well as to forecast the ionospheric weather up to hours ahead (ionospheric weather is much less predictable than tropospheric weather).

Ground-based GPS networks continuously provide global data for the derivation of quite accurate global and regional total electron content (TEC) maps. The results are obtained using a thin-shell model and data from many GPS sites (Mannucci et al. 1993). However, these results suffer from lack of knowledge about the vertical structure of the ionosphere. This can be dramatically improved by merging the ground-based data and ACE+ data, e.g. by using tomographic methods to estimate the 3D-structure of the free electrons (e.g. Ruffini et al. 1998). Combining all ground-based GPS/GALILEO data, available from 2008 onwards, with the large volume of ACE+ data will allow global and continuous analyses and forecasts of ionosphere and space weather of unprecedented quality.

References

Bony, S., K. M. Lau, and Y. C. Sud, 1997: Sea surface temperature and large-scale circulation influences on tropical greenhouse effect and Cloud Radiative Forcing, *J. Climate*, 10, 2055–2077.

Buehler, S.A., and N. Courcoux, 2003: The impact of temperature errors on perceived humidity supersaturation, *Geophys. Res. Lett.*, 30(14), 1759, doi:10.1029/2003GL017691.

European Space Agency, 1998: The Science and Research Elements of ESA's Living Planet Programme, ESA SP-1227, 105pp.

European Space Agency, 2001: WATS – Water Vapour and Temperature in the Troposphere and Stratosphere, ESA Publ., ESA, SP-1257(3). [online: http://www.estec.esa.int/granada_2001 > Assessment Reports]

Fjeldbo, G., A.J. Kliore, and V.R. Eshleman, 1971: the neutral atmospere of Venus as studied with the Mariner V radio occultation experiments, *Astron. J.*, 76, 123-140.

Foelsche, U., and G. Kirchengast, 2004: Sensitivity of GNSS occultation profiles to horizontal variability in the troposphere: a simulation study, *Proc. Book, 1st Int'l Workshop on Occultations for Probing Atmosphere and Climate (OPAC-1)*, Sept. 2002, Graz, Austria, Springer Verlag, in press. [online: http://www.uni-graz.at/igam-arsclisys > Publications]

Gage, K.S., 1990: Radar Observations of the Free Atmosphere: Structure and Dynamics, in *Radar in Meteorology* (Ed. D. Atlas), Part II, Chap 28, American Met. Society (AMS) Publ., 534–565.

GCOS, 2003: The Second Report on the Adequacy of the Global Observing Systems for Climate in Support of the UNFCCC, *WMO/TD No. 1143*, 74p., WMO, Geneva, Switzerland.

Gobiet, A., G. Kirchengast, J. Wickert, C. Retscher, D. Wang, and A. Hauchecorne, 2004: Evaluation of Stratospheric Radio Occultation Retrieval Using Data from CHAMP, MIPAS, GOMOS, and ECMWF Analysis Fields, *Proc. 2nd CHAMP Science Meeting, Sept. 2003*, Potsdam, Germany, Springer Verlag, in press.

Gorbunov, M.E., 2002: Canonical transform method for processing GPS radio occultation data in lower troposphere, *Radio Sci.*, 37, 9-1–9-10, doi:10.1029/2000RS002,592.

Gossard, E.E., 1990: Radar Research on the Atmospheric Boundary Layer, in *Radar in Meteorology,* Part II (Ed. D. Atlas), Chap 27, American Met. Society (AMS) Publ., 477–527.

Gradinarsky, L.P., P. Eriksson, and G. Elgered, 2003: ACEPASS Study – Analysis of the impact of clouds-rain-turbulence, *Draft Final ACEPASS WP4.3 Report*, 29p., Chalmers Univ. of Technology, Gothenburg, Sweden.

Hajj, G.A., E.R. Kursinski, L.J. Romas, W.I. Bertiger, and S.S. Leroy, 2002: A technical description of atmospheric sounding by GPS occultations, *J. Atmos. Sol.-Terr. Phys.*, 64, 451–469.

Hall, A. and S. Manabe, 1999: The role of water vapor feedback in unperturbed climate variability and global warming, *J. Clim.*, 12, 2327–2346.

Harries, J.E., 1997: Atmospheric radiation and atmospheric humidity, *Quart. J. Roy. Meteorol. Soc.*, 123, 2173–2186.

Healy, S. and J. Eyre, 2000: Retrieving Temperature, Water Vapour and Surface Pressure Information from Refractive Index Profiles Derived by Radio Occultation: A Simulation Study, *Quart. J. Roy. Meteorol. Soc.*, 126, 1661–1683.

Høeg, P., A. Hauchecorne, G Kirchengast, S. Syndergaard, B. Belloul, R. Leitinger, and W. Rothleitner, 1995: Derivation of Atmospheric Properties Using a Radio Occultation Technique, *Scient. Rep. 95-4*, DMI, Copenhagen, Denmark.

Høeg, P., and Ge. Leppelmeier, 2000: Atmosphere Climate Experiment, *Sci. Rep., DMI*, 00-01.

Høeg, P., and G. Kirchengast, 2002: ACE+ – Atmosphere and Climate Explorer based on GPS, GALILEO, and LEO-LEO radio occultation (ESA Earth Explorer Opportunity Mission Proposal), *Scient. Rep. 02-07*, DMI, Copenhagen, Denmark, and *Wissenschaftl. Ber. No. 14*, 121p., IGAM, Univ. of Graz, Austria, 2002. [online: http://www.uni-graz.at/igam-arsclisys > Publications]

IPCC, 2001: *Climate Change 2001: The Scientific Basis. Contribution of Working Group I to the Third Assessment Report of the Intergovernmental Panel on Climate Change* [Houghton, J.T., Y. Ding, D.J. Griggs, M. Noguer, P.J. van der Linden, X. Dai, K. Maskell, and C.A. Johnson (eds.)]. Cambridge University Press, Cambridge, United Kingdom and New York, USA, 881pp.

Jensen, A.S., M.S. Lohmann, H.-H. Benzon, and A.S. Nielsen, 2003: Full spectrum inversion of radio occultation signals, *Radio Sci.*, 38 , doi:10.1029/2002RS002,763.

Kirchengast, G., J. Hafner, and W. Poetzi, 1999: The CIRA86aQ_UoG model: An extension of the CIRA-86 monthly tables including humidity tables and a Fortran95 global moist air climatology model, *Techn. Report for ESA/ESTEC No. 8/1999*, 18p.,

Inst. Meteorol. Geophys., Univ. of Graz, Austria. [online: http://www.uni-graz.at/igam-arsclisys > Publications]

Kirchengast, G., J. Fritzer, and J. Ramsauer, 2002: End-to-end GNSS Occultation Performance Simulator Version 4 (EGOPS4) Software User Manual (Overview and Reference Manual), *Techn. Report for ESA/ESTEC No. 3/2002*, 472p., IGAM, Univ. of Graz, Austria. [online: http://www.uni-graz.at/igam-arsclisys > Publications]

Kirchengast, G., S. Schweitzer, J. Ramsauer, J. Fritzer, and M. Schwaerz, 2004a: Atmospheric Profiles Retrieved from ACE+ LEO-LEO Occultation Data: Statistical Performance Analysis using Geometric Optics Processing, *Draft Report, ESA contract No. 16743/02/NL/FF,* IGAM, Univ. of Graz, Austria. [online: ftp://ftp.estec.esa.int/pub/eopp/pub/ACEplus]

Kirchengast, G., J. Fritzer, M. Schwaerz, S. Schweitzer, and L. Kornblueh, 2004b: The Atmosphere and Climate Explorer Mission ACE+: Scientific Algorithms and Performance Overview, *Draft Report, ESA contract No. 16743/02/NL/FF,* IGAM, Univ. of Graz, Austria. [online: ftp://ftp.estec.esa.int/pub/eopp/pub/ACEplus]

Kirchengast, G., and P. Høeg, 2004: The ACE+ Mission: An Atmosphere and Climate Explorer based on GPS, GALILEO, and LEO-LEO Radio Occultation, *Proc. Book, 1st Int'l Workshop on Occultations for Probing Atmosphere and Climate (OPAC-1)*, Sept. 2002, Graz, Austria, Springer Verlag, in press. [online: http:// www.uni-graz.at/igam-arsclisys > Publications]

Kley, D., and J. M. Russel III, 1999: Plan for the SPARC water vapor assessment (WAVAS), *SPARC Newsletter No 13*, 5–8, July 1999.

Kursinski, E.R., G.A. Hajj, J.T. Schofield, R.P. Linfield and K.R. Hardy, 1997: Observing Earth's atmosphere with radio occultation measurements using the Global Positioning System, *J. Geophys. Res.*, 102, 23,429–23,465.

Kursinski, E.R., S. Syndergaard, D. Flittner, D. Feng, G. Hajj, B. Herman; D. Ward and T. Yunck, 2002: A microwave occultation observing system optimized to characterize atmospheric water, temperature and geopotential via absorption, *J. Atmos. Oceanic Technol.*, 19(12), 1897–1914.

Lee, L.-C., C. Rocken, and R. Kursinski (Eds), 2001: *Applications of Constellation Observing System for Meteorology, Ionosphere & Climate*, Springer Verlag, Hong Kong, 384pp.

Leroy, S., 1997: Measurements of Geopotential Heights by GPS Radio Occultation, *J. Geophys. Res.*, 102, D6, 6971–6986.

Liebe, H.J., G. Hufford, and M. Cotton, 1993: Propagation modelling of moist air and suspended water/ice particles at frequencies below 1000 GHz, in *52nd Specialists Meeting of the Electromagnetic Wave Propagation Panel*, p 542, AGARD.

Mannucci, A.J., B.D. Wilson, C.D. Edwards, 1993: A new method for monitoring the earth ionospheric total electron content using the GPS global network, *Proc. ION GPS-93*, 1323–1332.

Marquardt, C., and S. Healy, 2003: Validation of GRAS level 1b data, *EUMETSAT Report, WP 2.3*, EUMETSAT, Darmstadt, Germany.

Melbourne, W.G., E.S. Davis, C.B. Duncan, G.A. Hajj, K.R. Hardy, E.R. Kursinski, T.K. Meehan, L.E. Young, and T.P. Yunck, 1994: The application of spaceborne GPS to atmospheric limb sounding and global change monitoring, *JPL Publ. 94-18*, 147 pp., Jet Prop. Lab. Pasadena, Calif.

Nielsen, A.S., M.S. Lohmann, P. Høeg, H.-B. Benzon, A.S. Jensen, T. Kuhn, C. Melsheimer, S.A. Buehler, P. Eriksson, L. Gradinarsky, C. Jimenez, and G. Elgered, 2003: Characterization of ACE+ LEO-LEO Radio Occultation Measurements, *Draft Report, ESA contract no. 16743/02/NL/FF*. [online: ftp://ftp.estec.esa.int/pub/eopp/pub/ACEplus]

Park, M., W. J. Randel, D. E. Kinnison, R. R. Garcia, and W. Choi, 2004: Seasonal variation of methane, water vapor, and nitrogen oxides near the tropopause: Satellite observations and model simulations, *J. Geophys. Res.*, 109(D3), D03302, doi:10.1029/2003JD003706.

Rao, D.N., T. Narayana Rao, M. Venkataratnam, S. Thulasiraman, S.V.B Rao, P. Srinivasulu, and P.B. Rao, 2001: Diurnal and seasonal variability of turbulence parameters observed with Indian mesosphere-stratosphere-troposphere radar, *Radio Science*, 36(6), 1439–1457.

Rieder, M.J., and G. Kirchengast, 2001: Error analysis and characterization of atmospheric profiles retrieved from GNSS occultation data, *J. Geophys. Res.*, 106, 31,755–31,770.

Rocken, C., R. Anthes, M. Exner, D. Hunt, S. Sokolovskiy, R. Ware, M. Gorbunov, W. Schreiner, D. Feng, B. Herman, Y.H. Kuo, and X. Zou, 1997: Analysis and validation of GPS/MET data in the neutral atmosphere, *J. Geophys. Res.*, 102, 29,849–29,866.

Rodgers, C., 2000: *Inverse methods for atmospheric sounding: theory and practice*, 256 pp., Word Sci., River Edge, N.J.

Roeckner, E., L. Bengtsson, J. Feichter, J. Lelieveld, and H. Rodhe, 1999: Transient climate change simulations with a coupled atmosphere-ocean GCM including the tropospheric sulfur cycle, *J. Climate*, 12, 3004–3032.

Ruffini, G., A. Flores, and A. Rius, 1998: GPS tomography of the ionospheric electron content with a correlation functional, *IEEE Trans. Geosci. Rem. Sens.*, 36.

Schrøder, T., S. Leroy, M. Stendel, and E. Kaas, 2003: Validating the Microwave Sounding Unit Stratospheric Record Using GPS Occultation, *Geophys. Res. Lett.*, 30(14), 1734–1737.

Smith, E.K. and S. Weintraub, 1953: The constants in the equation of atmospheric refractive index at radio frequencies, *Proc. I.R.E.*, 41(8), 1035–1037.

Soden, B.J., and J.R. Lanzante, 1996: An Assessment of Satellite and Radiosonde Climatologies of Upper-Tropospheric Water Vapor, *Journal of Climate*, 9, 1235–1250.

Soden, B.J., D.D. Turner, B.M. Lesht, L.M. Miloshevich, 2004: An analysis of satellite, radiosonde, and lidar observations of upper tropospheric water vapor from the Atmospheric Radiation Measurement Program, *J. Geophys. Res.*, 109(D4), D04105, doi: 10.1029/2003JD003828.

Sokolovskiy, S.V., 2001: Tracking tropospheric radio occultation signals from low earth orbit, *Radio Sci.*, 36 , 483–498.

SPARC, 2000: Assessment of Upper Tropospheric and Stratospheric Water Vapour, *WCRP-113, WMO/TD No.1043, SPARC Report No.2.*, December 2000.

Spichtinger, P., K. Gierens, and W. Read, 2002: The statistical distribution law of realtive humidity in the global tropopause region, *Meteorologische Zeitschrift*, 11, 83–88.

Steiner, A.K., G. Kirchengast, and H.P. Ladreiter, 1999: Inversion error analysis and validation of GPS/MET occultation data, *Ann. Geophys.*, 17, 122–138.

Steiner, A.K., G. Kirchengast, U. Foelsche, L. Kornblueh, E. Manzini, and L. Bengtsson, 2001: GNSS occultation sounding for climate monitoring, *Phys. Chem. Earth (A)*, 26, 113–124.

Steiner, A.K., and G. Kirchengast, 2004: Ensemble-based analysis of errors in atmospheric profiles retrieved from GNSS occultation data, *Proc. 1st Int'l Workshop on Occultations for Probing Atmosphere and Climate (OPAC-1)*, Sept. 2002, Graz, Austria, Springer Verlag, in press. [on-line: http://www.uni-graz.at/igam-arsclisys > Publications]

Syndergaard, S., 1999: Retrieval analysis and methodologies in atmospheric limb sounding using the GNSS radio occultation technique, *DMI Sci. Rep. 99-6*, 131 pp., Danish Meteorological Inst., Copenhagen, Denmark.

Syndergaard, S, D. Flittner, R. Kursinski, D. Feng, B. Herman and D. Ward, 2004: Simulating the influence of horizontal gradients on retrieved profiles from ATOMS occultation measurements: a promising approach for data assimilation, *Proc. 1st Int'l Workshop on Occultations for Probing Atmosphere and Climate (OPAC-1)*, Sept. 2002, Graz, Austria, Springer Verlag, in press.

Vasseur, H., 1999: Prediction of tropospheric scintillation on satellite links from radiosonde data, *IEEE Trans. Ant. Prog.*, AP-47(2), 293–301.

Vedel, H., and M. Stendel, 2004: GPS RO Refractivities as a Climate Change Measure, submitted to *Climatic Change*.

WMO, 1996: CBS Working Group on Satellites, Second Session, 15–19 April 1996, *Final Report. WMO*, Geneva.

WMO, 2000a: *Technical Document No. 992*, SAT-22, April 2000.

WMO, 2000b: *CEOS/WMO Database* (CD-ROM). September 2000.

Yuan, L.L., R.A. Anthes, R.H. Ware, C. Rocken, W.D. Bonner, M.G. Bevis, and S. Businger, 1993: Sensing Climate Change Using the Global Positioning System, *J. Geophys. Res.*, 98(D8), 14,925–14,937.

Zou, X., F. Vandenberghe, B. Wang, M. Gorbunov, Y.-H. Kuo, S. Sokolovsky, J. Chang, J. Sela, C. Lee and R. Anthes, 1999: A raytracing operator and its adjoint for the use of GPS/MET refraction angle measurements, *J. Geophys. Res.*, 104, 22,301–22,318.

Acronyms

ACE+	Atmosphere and Climate Explorer
AIRS	Atmospheric InfraRed Sounder
AMSU	Advanced MSU
BLUE	Best Linear Unbiased Estimation
CEOS	Committee on Earth Observation Systems
CHAMP	CHAllenging Minisatellite Payload
CLIVAR	Climate Variability and predictability – an international research programme under WCRP
COSMIC	Constellation Observing System for Meteorology, Ionosphere, and Climate
COST	European Co-operation in the field of Scientific and Technical Research (intergovernmental framework)
ECMWF	European Centre for Medium-range Weather Forecasts
ENSO	El Nino/Southern Oscillation
EOEP	Earth Observation Envelope Programme
EPS	EUMETSAT Polar System
ERA-40	ECMWF's re-analysis project covering the period 1957 to 2001
ESWP	European Space Weather Programme
EUMETNET	The network of European meteorological services
EUMETSAT	EUropean organisation for the exploitation of METeorological SATellites
GALILEO	European future global navigation satellite system
GCM	Global Circulation Model
GCOS	Global Climate Observing System
GEWEX	Global Energy and Water cycle EXperiment – an international research programme under WCRP
GLONASS	Russian global navigation satellite system
GMES	Global Monitoring for Environment and Security
GNSS	Global Navigation Satellite System (generic term for GPS, GALILEO, GLONASS)
GOS	Global Observing System
GPS	Global Positioning System (USA)
HALOE	HALogen Occultation Experiment
HIRS	High-resolution Infrared Radiation Sounder
IASI	Infrared Atmospheric Sounding Interferometer
ICSU	International Council for Science
IGS	International GPS Service
IOC	Intergovernmental Oceanographic Commission of UNESCO
IPCC	Intergovernmental Panel on Climate Change
K-band	Microwave frequency region 18-26 GHz (Ku: 12-18 GHz)
L-band	Microwave frequency region 1-2 GHz
LEO	Low-Earth Orbit

MAG	Mission Advisory Group
MetOp	Meteorological polar-orbiting satellite. European operational weather satellite to be launched in 2005
MLS	Microwave Limb Sounder
MPM	Millimetre-wave Propagation Model(s)
MSU	Microwave Sounding Unit
NOAA	National Oceanographic and Atmospheric Administration (USA)
NPOESS	National Polar-orbiting Operational Environmental Satellite System (USA)
NWP	Numerical Weather Prediction
OPS	Observation Processing System
OSE	Observation System Experiment
POD	Precise Orbit Determination
RMS	Root Mean Square
RO	Radio Occultation
SPARC	Stratospheric Processes And their Role in Climate – an international research programme under WCRP
SSM/I	Special Sensor Microwave/Imager
TEC	Total Electron Content
TIROS	Television and InfraRed Observation Satellite
TOVS	TIROS Operational Vertical Sounder
UARS	Upper Atmosphere Research Satellite
UNEP	United Nations Environmental Programme
USO	Ultra Stable Oscillator
UTLS	Upper Troposphere and Lower Stratosphere
WATS	WAter vapour and temperature in the Troposphere and Stratosphere (previous GNSS-LEO and LEO-LEO RO satellite constellation mission proposal to ESA)
WCRP	World Climate Research Programme
WMO	World Meteorological Organization
WWW	World Weather Watch
X-band	Microwave frequency region 8-12 GHz

European Space Agency
Agence spatiale européenne

Contact: ESA Publications Division
c/o ESTEC, PO Box 299, 2200 AG Noordwijk, The Netherlands
Tel. (31) 71 565 3400 - Fax (31) 71 565 5433